The conductance of ballistic rings

Thesis submitted in partial fulfillment of the requirement for the degree of master of science in the Faculty of Natural Sciences

Submitted by: **Yoav Etzioni**

Advisor: **Prof. Doron Cohen**

Department of Physics

Faculty of Natural Sciences

Ben-Gurion University of the Negev

December 25, 2006

Abstract

The Landauer conductance, the conductance of open mesoscopic systems, equal in the weak scattering limit to the number of open modes. In this work we will ask what is the corresponding result if we close the system into a ring. Will it still be bounded by the number of open modes? We have found two results for this question. The first one [1] applies if we assume very short coherence time, therefore the treatment is essentially classical one. Using a scattering approach we find an expression for the conductance, which we call the Drude conductance. We will also make a distinction between various environmental effect and analyze a model for a multimode ring with a specific scatterer and demonstrate that unlike the conductance for an open system, in closed system the conductance is not bounded by the number of open modes.

In the second part of our work [2] we will consider an essentially coherent ring where driving cause weak level broadening, as a result energy absorption due to Fermi golden rule transitions occur. We find that if the environmental induce relaxations processes are much weaker compare to the driving, the result will be a new type of conductance which we named mesoscopic conductance. That conductance is much smaller compared with the classical one, this is a result of nonuniversal structures of the perturbation matrix, which are a generic ingrediant for quantum chaotic systems.

The conductace is define via Jouls law, as the coeffecient of energy dissipation rate, and the nonuniversal structures, or sparcity in the matrix may create bottelnecks that suppress the dissipation. We determine the conductance using the analogy with percolation problem, only in our case the percolation is in energy space. We also make a distinction between this mesoscopic conductance to the much larger spectroscopic conductance which is created if the relaxations processes are stronger.

In the third part of our work we have varify the generality of our statement by analyzing a realistic model in which the ring is modeled as a waveguide with a semidisc scatterer.

The main parts of this work are contained in:

[1] D. Cohen and Y. Etzioni,
"The multi-mode conductance formula for a closed ring"
J. Phys. A **38**, 9699 (2005).

[2] Y. Etzioni, S. Bandopadhyay and D. Cohen,
"The mesoscopic conductance of ballistic rings"
cond-mat/0607746, submitted to J.Phys.A

[3] S. Bandopadhyay, Y. Etzioni, and D. Cohen,
"The conductance of a multi-mode ballistic ring: beyond Landauer and Kubo"
cond-mat/0603484, Europhysics Letters [In Press]

Contents

Chapter 1

Introduction

The theory for the conductance of closed mesoscopic rings [4, 5, 6, 7, 8, 9] has attracted a lot of interest in past years. In a typical experiment [10] a collection of mesoscopic rings are driven by a time dependent magnetic flux $\Phi(t)$ which creates an electro-motive-force (EMF) $-\dot{\Phi}$ in each ring. Assuming that Ohm's law applies, the induced current is $I = -G\dot{\Phi}$ and consequently Joule's law gives

$$\text{Rate of energy absorption} \quad = \quad G\,\dot{\Phi}^2 \tag{1.1}$$

where G is called the conductance. For diffusive rings the Kubo formula leads to the Drude formula for G. A major challenge in past studies was to calculate the weak localization corrections to the Drude result, taking into account the level statistics and the type of occupation [9]. It should be clear that these corrections do not challenge the leading order Kubo-Drude result.

It is just natural to ask what is the conductance if the mean free path ℓ increases, so that we have a ballistic ring, where the total transmission is $g_T \sim 1$. To be more precise, we assume that the mean free path

$$\ell \quad \approx \quad \frac{1}{1 - g_T}L \tag{1.2}$$

is much larger than the perimeter L of the ring. In such circumstances "quantum chaos" considerations become important.

We want to make clear distinction between classical and quantal effects. This helps to develop a better intuition for the physics of such devices. Here "classical" as opposed to "quantum" should be understood in the sense of Boltzmann picture. In the "classical" case the interference within the arm of the ring is ignored, while both the Fermi statistics and the single scattering events are treated properly.

In the first part of this work we are interested in circumstances such that the leading result for the conductance is of classical nature. This is completely analogous to the discussion of *diffusive* rings in circumstances such that the leading result is given by the Drude formula. We are going to assume that the coherence time is much shorter than the time that it takes for an electron to encircle the ring. Thus, as far as the dynamics is concerned, our analysis is essentially of *classical* nature.

The approach in this part is that the scattering "cross section", which is possibly of quantum mechanical nature, is taken as an input, while the overall dynamics is assumed to be of classical nature.

In the second part of this work we will discuss the implications of quantum interference. Following [11] we argue that the calculation of the energy absorption in Eq.(1.1) is somewhat similar to solving a percolation problem. The "percolation" is in energy space rather than in real space. This idea was further elaborated in [12].

In the standard derivation of the Kubo formula [13] it is assumed that the leading mechanism for absorption is Fermi-golden-rule transitions. These are proportional to the squared matrix elements $|\mathcal{I}_{nm}|^2$ of the current operator. Still, the theory of [11] does not lead to the Kubo formula. This is because the rate of absorption depends crucially on the possibility to make *connected* sequences of transitions, and it is greatly reduced by the presence of bottlenecks. It is implied that both the structure of the $|\mathcal{I}_{nm}|^2$ band profile and its sparsity play a major role in the calculation of G. This issue will also be treated by the

7

scattaring approach, using S matrix.

This approach to the problem of conductance has a *practical appeal.* The reason for the popularity of the scattering approach in mesoscopic physics is its "plug and play" feature. The experimentalist is able to characterize the scattering properties of his/her device, and then he/she is able to make a prediction regarding the conductance. It is only natural to extend this "plug and play" approach to the analysis of conductance of *closed* rings. This extension is far from being trivial.

In the second part of the work we will consider a schematic S matrix which couple several bonds in a ring geometry. In the last part of this work we analyze a more realistic model. In that part of the work we will consider a waveguide, close to a ring, which support several open channels. We find an S matrix which describe a semi disc shaped scatterer which couple those modes together. We will show that all the main ingredients in the calculation of he conductance can be found in our previous, simplified model.

1.1   The long time scenario

Some people find it inappropriate to define conductance for a closed system because the problem does not possess a stationary solution. Namely, it is clear that without a contact to a thermal bath the driven system is gradually heated up. However, we find this objection of no relevance. The practical point of view of an electrical engineer is demonstrated in Fig.1c. It is clear that at any *moment* the engineer is inclined to characterize the ring by its conductance. This is true irrespective of whether there is a contact with a thermal bath or not. In the absence of such contact it is evident that the system is heated up and therefore the conductance becomes time-dependent.

It is true that the overall scenario is (formally) beyond linear response, but it is also true that at a given instant of time it is feasible to have a valid linear response description. The validity condition is having an ergodization time which is much smaller than the time

that it takes to have a significant change in the (evolving) energy distribution of the system. This reasoning leads to "slowness conditions" that are further discussed in Ref.[13].
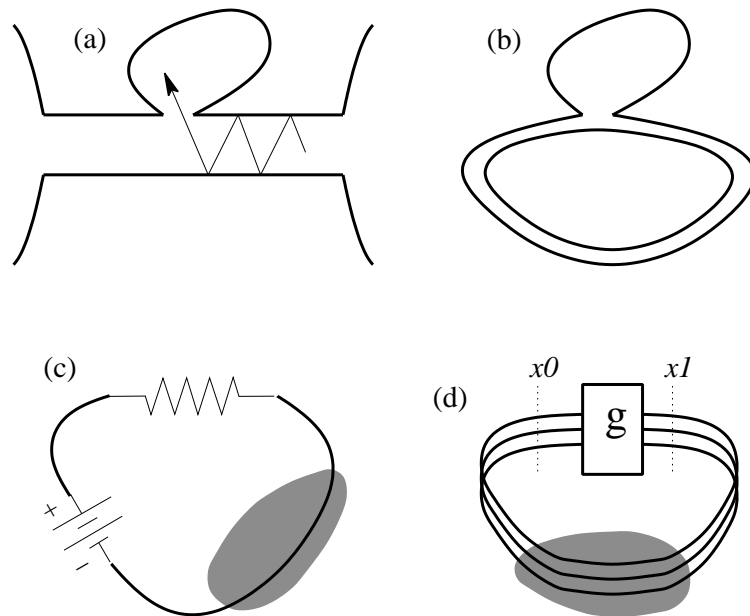
Fig.1 Panel (a) displays the standard Landauer (open) geometry of connecting a conductor to a left and a right reservoirs. In this illustration the conductor is a rectangular waveguide to which a cavity is attached. In panel (b) the leads are joined together so as to form a ring. The motion in the ring is assumed to be chaotic due to the scattering in and out of the cavity. Panel (c) is the schematic electrical engineering representation of the system. In panel (d) the system is modeled as a network. The scattering region is described by the transition matrix g_{ab}. In (c) and in (d) we indicate the presence of the environment by the gray shading. In fact (a) can be regarded as a special case of (b) provided one assumes that the effect of the environment is to randomize the velocity within the wire region. The current is measured via the section $x = x_1$. The Electro motive force (EMF) is realized by time dependent Aharonov Bohm flux. The voltage drop can be concentrated anywhere along the ring (say across $x = x_0$). Setting a chemical potential difference in the setup of panel (a) can be regarded as such particular option.

1.2   Relation of the work to past works

In this section we will clarify on the physical conditions assumed in our work and their relation to other works. we begin with the following scheme which present the energy as a function of the mean free path l (the elastic length).
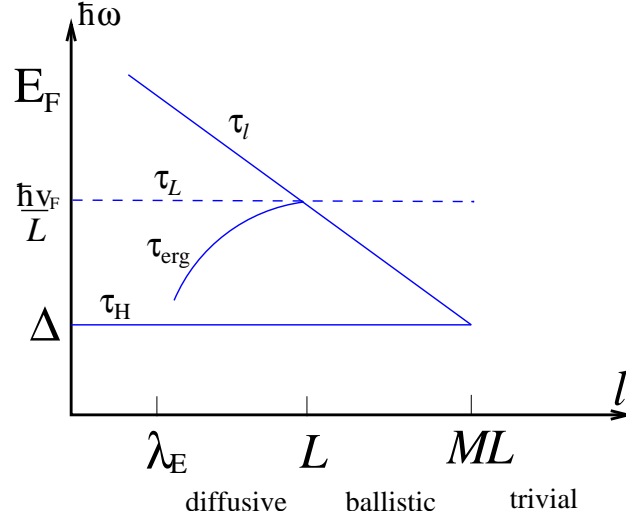
Fig.2 Energy and time scales in the diffusive and ballistic regimes

where $\tau_l = l/v_F$ is the mean free time, v_F is the Fermi velocity. $\tau_L = L/v_F$ is the time for encircling the ring, the inverse of the level spacing of a single mode. τ_H is the Heisenberg time, the inverse of the level spacing. Using the Fermi velocity we can characterize those time scale either by their characteristic lengths or their energy scales.

$\tau_{\mathrm{erg}} = L^2/D$ is the ergodic time. It describe the time it take for an electron to spread out in the system, where $D = l^2/\tau_l$ is the diffusion coefficient. This time scale, also known as the Thouless time is an important time scale in the physics of diffusive conductors. Our work in focused on the ballistic regime in which the mean free path is

$$L \ll l \ll \mathcal{M}L \tag{1.3}$$

Two other regimes are, the trivial regime where $\mathcal{M}L \ll l$ in which there is no mixing of modes, and as a result the conductance of the ring in mesoscopic conditions will vanish, this

issue is explained in section 4.10.

The diffusive regime, where $l \gg L$ has been studied extensively. In a review by Kmenev and Gefen [9] the authors considered the case of a closed diffusive system. They emphasis that for a diffusive system the leading order results for the conductance are the Drude results, plus other, weak localization corrections. Where the Drude results are the Thouless energy, the inverse of τ_{erg}, divided by the mean level spacing [[42]], and the quantum corrections reduce the conductance of the system.

The authors analyze in there work the conductance of a close diffusive systems, and the conductance dependence on flux. They found that two ingredients are crucial for this analysis. First, the ratio between the mean level spacing and the inelastic broadening, the broadening of the level due to coupling to an outside environment. They distinguish between the continuous spectrum limit, due to the level broadening, and the discrete spectrum limits. Second, the emphasis the importance of the type of statistical ensemble employed, they distinguish between canonical and grand canonical ensembles. In their work the authors stress that of the two common approaches for calculating the conductance of a quantum system, the Landauer approach and the Kubo approach, only the latter is suitable when considering a leadless geometry.

The relation among the important energy scales in the diffusive regime, as can be seen clearly in the above figure are as follow.

$$\Delta \ll {\tau_{\mathrm{erg}}}^{-1} \ll {\tau_l}^{-1} \ll E_F \tag{1.4}$$

Those energy/time scales are related to the geometry of the system.

We will clarify on the effect of the environment and the driving on the system's behavior. We consider two relevant energy scale, the first one is Γ, which describe the broadening of the levels due to non adiabatic driving, or due to interaction with a noisy environment, we elaborate on this issue in chapter 2. This Γ can be also describe by its characteristic length the coherence length.

11

In the first part of our work, chapter 3 we assume that this length is very short, so we can treat the problem as a classical one, while ignoring interference effects, this issue is discussed in 1.3.

In the main part of our work, chapters 4 and 5 we treat Γ as a phenomenological parameter which is larger then the mean level spacing Δ, so we have some level broadening, but still the level are not smeared. So Γ is still much smaller then $\Delta_b = \mathcal{M}\Delta$, the energy scale related to the time scale τ_L. Conductance will be the result of transitions between energy levels due to this parameter. We elaborate on this issue in section 2.3.

The second relevant energy scale is that of the relaxation γ_{rlx}. It describe the release of energy in the system to the environment, its characteristic time is the inelastic time.

We explain this physical picture in the following diagram. On the one hand the driving source induce transitions between energy levels of the system, leading to absorption of energy with some rate $\dot{\mathcal{W}}$ which depend on the level broadening parameter Γ. On the other hand the system can release energy to the environment, which lead to a "heat flow" with some rate $\dot{\mathcal{Q}}$, this depend on γ_{rlx}.

In the lower panel we plot how $\dot{\mathcal{W}}$ depends on time. If γ_{rlx} is small enough then there is transient to a slower absorption rate. This issue will be explained in 4.4.
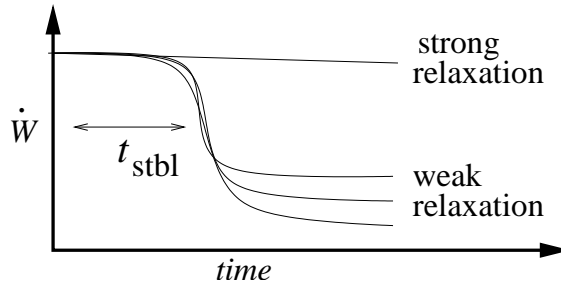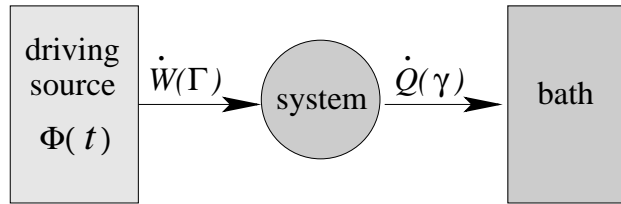
Fig.3 The phenomenology of energy absorption

Two other, rival, dissipation mechanisms, that should be mentioned are the Landau-Zener transition [8] and the Debye relaxation [5]. Both mechanisms describe condition where the mean level spacing Δ is larger the both Γ and γ_{rlx}. Landau-Zener describe conditions where

$$\gamma_{\mathrm{rlx}} \ll \Gamma \ll \Delta \tag{1.5}$$

In this case the main source for dissipation are transitions between pairs of nearly degenerate energy level. As the energy levels are change with the change of some driving parameter X, there are regions in X, where the level spacing is very small. Those regions, the avoided crossings, enable transition even when $\Gamma \ll \Delta$.

Debye relaxation mechanism describe condition where

$$\Gamma \ll \gamma_{\mathrm{rlx}} \ll \Delta \tag{1.6}$$

In this case the environment induce relaxation processes which result in a Boltzmann distribution of particle among the energy levels. Changing the parameter X will change the distribution of energy levels, as the inelastic relaxation time is much shorter compared with the adiabatic variation of the energy levels a time lag between the driving and the adjustment of the occupation probabilities will cause dissipation in the system.

In our case we assume that the broadening parameter Γ is larger then the mean level spacing Δ, and Fermi golden rule transitions cause the dissipation. We also assume that $\gamma_{\mathrm{rlx}} \ll \Gamma$. So the release of energy to the environment is negligible. the traditional Kubo derivation assumes $\Delta \ll \gamma_{\mathrm{rlx}}$. This is explained in section 4.4.

Some authors describe the contributions to the conductance as either diagonal, when the particles remain on the same energy levels, as in Debye relaxation. or off-diagonal where the conductance is a result of levels transitions as in Landau-Zener and also in our system, where Fermi golden rule transitions are the source of dissipation.

13

1.3 The role of the environment

In this section we will clarify the different physical circumstances we consider for the case of a semiclassical calculation. Our first step is to define a feasibility condition for the validity of a semiclassical treatment. Assuming that the total transmission of the device is $g_T \sim 1$ the time for the randomization of the velocity is

$$\tau_{cl} \approx \left(\frac{1}{1 - g_T} \right) \times \frac{L}{v_F} \qquad (1.7)$$

where L is the length of the ring, and v_F is the Fermi velocity. On the other hand the time that it takes to resolve the quantized energy levels of the ring is

$$t_{\text{Heisenberg}} \approx \mathcal{M} \times \frac{L}{v_F} \qquad (1.8)$$

Where $\mathcal{M}$ is the number of open modes. Hence the quantum-to-classical correspondence condition is

$$\mathcal{M} \gg \frac{1}{1 - g_T} \qquad (1.9)$$

which is always satisfied in the classical limit. Note that the limit $\mathcal{M} \to \infty$ is analogous to $\hbar \to 0$.

In the case of a single mode ring (a one dimensional ring with a delta scatterer) a classical treatment of the dynamics does not make any sense in view of the correspondence condition. The analysis should be purely quantum mechanical issues such as Landau-Zener transitions [8], Debye relaxation mechanism [5] should be taken into account.

In the case of multi mode diffusive ring the leading order result for the conductance is as expected just the classical Drude expression. The typical calculation [6] assumes that the levels are "broadened" due to the interaction with the environment. In the major case of interest the level broadening Γ is assumed to be larger than the mean level spacing Δ but much smaller than any semiclassical energy scale. Hence it barely affects the Drude result. Still it determines the quantum weak localization correction, which are of the order

Δ/Γ. The weak localization correction depends on the levels statistics and therefore on the magnetic flux. Hence it can be detected in an actual experiment [10].

In chapter 3 We consider a multi mode ballistic ring rather than a diffusive ring. This means that the time to randomize the velocity can be much larger than the time L/v_F to make one round along the ring. This implies that in our configuration the conductance (in natural units) can be larger than the number of open modes.

We assume that the environment induces level broadening Γ which is larger than $\hbar v_F/L$. Hence we derive the leading (classical) term and do not take into account the implications of quantum interference. To put this assumption in a larger perspective we make the following classification:

1. Isolated system (no environment).

2. The bath induces only decoherence effect.

3. The bath induces velocity randomization.

4. Bath limited dynamics.

The first case of fully coherent dynamics will be analyzed in chapter 4. We would like to further explain why the second case is physically typical, and to make some comments on the other two cases.

It is typical to assume that the fluctuations of the environment are of large spatial correlation length compared with W, the width of of the waveguide. An extreme case is the Caldeira-Leggett modeling which assumes an infinite correlation length. The matrix elements of the position variable scale like W for inter-mode transitions and like L for intra-mode transitions. Hence inter-mode transitions are rare compared with intra-mode transitions, the ratio being $(W/L)^2$. Therefore it is realistic to consider circumstances such that velocity randomization due to the environmental "noise" can be neglected, while intra-mode transitions cannot be neglected. The latter lead to decoherence. The simplest estimate for the

decoherence rate is $\Gamma = \eta k_B T L^2 / \hbar$, where η characterizes the coupling to the environmental modes, and T is the temperature. Thus we see that case 2 is physically typical.

If the fluctuations are strong enough inter-mode transitions cannot be ignored. This would lead to randomization of the velocity in the wire region. The scenario of having a bath that just randomizes the velocity, but does not affect the transmission of the ring is apparently not of much physical interest. Still such effect can be realized artificially, and it is of pedagogical importance, it will be discuss in section 3.5.

If the interaction with the environment determines the transmission of the ring, we get to case 4. The most obvious example is the analysis of conductance in room temperatures. The scattering and hence the diffusion of the particles is dominated by bath induced inelastic scattering by phonons.

The main point regarding case 4 is that the bath cannot be eliminated from the model analysis. Another example for such circumstances is provided by the Debye dissipation mechanism.

1.4   Wavefunction statistics

Quantum graphs, have been used successfully for many years as simple dynamical systems in which to study complex wave behavior. For appropriate parameter values, graphs can be made to display generic chaotic, disorder, or integrable motion, and at the same time the quantum mechanics of this systems has the simplifying advantage of being semiclassically exact.

Quantum graph is a system of vertices, connectend by a one dimensional bonds on which an electrons can travel from one bond to another, and scattered by the vertices. A Sinai billiard is one example in which quantum graphs is used, where different modes are represented by the various bonds.

The statistics of the eigenfunction in such system has long been studied. In an early

work Berry [15] conject that the quantum eigenfunctions of a classical chaotic system look like a random superposition of plane waves with fixed energy. contrary to that Heller [16] has developed the scar theory, which state that many eigenfunctions in the system display a concentration of amplitude around short classical unstable periodic orbits, which result in excess density much greater then that expected by the fluctuation in random matrix theory.

One has to distinguish between scarring in the intensities for an energy window of nearby eigenstate, meaning scarring in the position representation. Bogomolny [17] has computed an expression for scar intensity in that representation.

A diffrent case is scarring in an individual eigenstate in which a single, or a few bonds has a very large intensity, while all other bonds are very weak. Agam & Fishman [18] developed a criterion for predicting scarring. Bäker & Schuber suggest considering scars in momentum space [19].

A theorem by Schnirelma [20] stated that the classical expectation value converge to the microcanonical average, this is in agreement with scarring because the size of the scar scale ha $\hbar$ and therefore vanish in the semiclassical limit.

Kaplan & Heller [21] has extended the theory of scars to the nonlinearizeable regime, there claim is that scarring is a weak localization phenomenon that occur when a wave packet centered on the unstable periodic orbit overlaps with the eigenstate of the system. They have also claim [22] that even without considering scars, the total amount of localization in a billiard is much larger then that expected by random fluctuation. Berkolaiko, Keating & Winn [23] reach similar conclusions when they study billiard chaotic systems. Schanz & Kottos [24] have shown that short periodic orbit and scarring can, in principle rely on different mechanisms.

1.5 Outline

In chapter 2 we discuss the issue of linear response and Kubo formula, it will be explained that the purpose of the "linear response analysis" is to find the stationary-like state of the driven system. The procedure is to assume that in the absence of driving the system would be in a (strict) stationary state, which we regard as the zero order solution. Then we try to find a first order solution (in the EMF) to the time dependent problem.

In sections 2.1 and 2.2 we discuss the Kubo approach to linear response. We take the simplest route following Refs.[8, 13, 27, 28] leading to the fluctuation-dissipation version of the Kubo formula.

In section 2.3 we outline the procedure used in the calculation of the conductance in circumstances such that the motion inside the ring is coherent (quantum interference within the bonds is not ignored).

In chapter 3 we present the main work done in [1]. We define the model system in sections 3.1 and 3.2. In sections 3.3 and 3.4 we present the application of the Kubo formula to the analysis of the single mode conductance, The relation to the Landauer result is clarified in section 3.5.

We show that the conductance of a single mode ring ($\mathcal{M} = 1$) with a stochastic scatterer that has transmission g_T is given by the expression which we call the Drude conductance

$$G_{\text{Drude}} = \frac{e^2}{2\pi\hbar} \left[\frac{g_T}{1 - g_T} \right] \tag{1.10}$$

It turns out that the derivation of the multi-mode conductance formula becomes more transparent by adopting a master equation approach. This is carried out in section 3.6. with the results that the generalization of last formula is:

$$G_{\text{Drude}} = \frac{e^2}{2\pi\hbar} \sum_{nm} \left[2g^T / (1 - g^T + g^R) \right]_{nm} \tag{1.11}$$

where g_{nm}^T and g_{nm}^R are the $\mathcal{M} \times \mathcal{M}$ transmission and reflection blocks of the transition matrix.

In section 3.7 we analyze a specific example for a scatterer, a cavity connected to a closed wire (Fig.1a) and find that unlike the case of the Landauer conductance, the result does not reflect the number of open modes. This is because the contribution of the low modes is singular in the limit of small α. Furthermore, the conductivity (conductance per channel) diverges logarithmically in the classical limit. The Landauer results

$$G_{\text{Landauer}} \approx \frac{e^2}{2\pi\hbar} \left[1 - \frac{1}{4}\alpha \right] \mathcal{M} \tag{1.12}$$

where α is the dimensionless size of the opening to the cavity. In contrast to that for the Drude conductance of the corresponding ring structure (Fig.1b) is

$$G_{\text{Drude}} \approx \frac{e^2}{2\pi\hbar} \left[\frac{1}{\alpha}(1 + \ln(2\mathcal{M})) \right] \mathcal{M} \tag{1.13}$$

In chapter 4 we present the main work done in [2]. We will discuss the modeling of ballistic rings, clarify the procedure which is involved in the calculation of the conductance, and analyze the simplest example.

In sections 4.1 we distinguish between

- Disordered rings (e.g. Anderson model)

- Chaotic rings (e.g. billiard systems)

- Network models (also known as "graphs")

In particular we motivate the analysis of a simple prototype network model for a multimode ring. This model has all the essential ingredients to demonstrate the major theme of this paper.

In sections 4.2-4.5 we continue with the procedure which is used for the calculation of the conductance. This is not merely a technical issue, since new concepts [11, 12] are involved. We make a distinction between:

- The previous classical results

- The (quantum) spectroscopic conductance of a ring

- The (quantum) mesoscopic conductance of a ring

for a prototype model we get the following results: Given that the device has $\mathcal{M}$ open modes and its total transmission is $g_T < 1$, the Landauer conductance is [29]

$$G_{\text{Landauer}} = \frac{e^2}{2\pi\hbar}\mathcal{M}\ g_T \tag{1.14}$$

The Drude result for the closed ring is

$$G_{\text{Drude}} = \frac{e^2}{2\pi\hbar}\mathcal{M}\ \frac{g_T}{1 - g_T} \tag{1.15}$$

and the associated quantum results are

$$G_{\text{spec}} \approx \frac{e^2}{2\pi\hbar}\mathcal{M} \times \text{maximum}\left[\frac{g_T}{1 - g_T}, \mathcal{M}\right] \tag{1.16}$$

$$G_{\text{meso}} = \frac{e^2}{2\pi\hbar}\ 2\mathcal{M}^2\ \mathbf{g}_{\text{meso}} \tag{1.17}$$

The calculation of $\mathbf{g}_{\text{meso}}$ involves a complicated *coarse graining* procedure that we discuss in section 4.5. The spectroscopic result G_{spec} describes via Eq.(1.1) both the initial (transient) rate and also the long time (steady state) rate of energy absorption, provided the environment provides a strong relaxation mechanism. The mesoscopic result describes the (slower) long time rate of energy absorption if the environmentally induced relaxation is weak. See [11] for an extended quantitative discussion.

The outcome for G_{meso} may differ by orders of magnitude from the conventional Kubo-Drude result. The calculation procedure implies that $G_{\text{meso}} < G_{\text{spec}} \leq G_{\text{Drude}}$. In sections 4.6-4.10 we demonstrate this point via the analysis of the prototype model. Our numerical results suggest that typically $G_{\text{meso}} < G_{\text{Landauer}}$. The results of the calculation are contrasted with those of the conventional Kubo approach,

In chapter 5 we will repeat the calculation for this more realistic model, in order to show that the results obtained are applicable to

In section 5.1 we describe the waveguide model and its properties. We will calculate the classical probabilities transitions, the $\boldsymbol{g}$ matrix. We continue with the quantum S matrix in section 5.2, and compare those results in section 5.3. In sections 5.4 and 5.6 we will use that S matrix for the calculation of the matrix elements in the Kubo formula. We will discuse the result in section 5.7.

Chapter 2

Linear response theory

The simplest route to linear response theory [8, 13, 27, 28] takes the relation $d\mathcal{H}/dt = \partial\mathcal{H}/\partial t$ as a starting point. It follows that the change in the energy of a particle is given with no approximation by the formula

$$\mathcal{H}(t) - \mathcal{H}(0) = -\dot{\Phi}\int_0^t \mathcal{F}(t')dt' \tag{2.1}$$

By squaring and averaging over initial conditions we get that the second moment as a double time integral over $\langle\mathcal{F}(t')\mathcal{F}(t'')\rangle$. Within linear response this correlation is *approximated* by the *stationary* correlation function

$$C(t' - t'') = \langle\mathcal{F}(t')\mathcal{F}(t'')\rangle_E \tag{2.2}$$

where the average on the right hand side is taken with a zero order microcanonical solution. Thus one concludes that there is a diffusion in energy, with the coefficient

$$D_E = \dot{\Phi}^2 \times \frac{1}{2}\int_{-\infty}^{\infty} C(\tau)d\tau \tag{2.3}$$

Next one wants to see what happens in the more general case of an arbitrary $f(E)$. On long times it is argued that the probability distribution $\rho(E)$ satisfies the following diffusion equation:

$$\frac{\partial\rho}{\partial t} = \frac{\partial}{\partial E}\left(\mathrm{g}(E)D_E\frac{\partial}{\partial E}\left(\frac{1}{\mathrm{g}(E)}\rho\right)\right) \tag{2.4}$$

The energy of the system is $\langle \mathcal{H} \rangle = \int E\rho(E)dE$. It follows that the rate of energy absorption is

$$\frac{d}{dt}\langle \mathcal{H} \rangle = -\int_0^\infty dE \; \mathsf{g}(E) \; D_E \; \frac{\partial}{\partial E}\left(\frac{\rho(E)}{\mathsf{g}(E)}\right) \tag{2.5}$$

For zero temperature Fermi occupation we get

$$\frac{d}{dt}\langle \mathcal{H} \rangle \;=\; \Big[\mathsf{g}(E)\,D_E\Big]_{E=E_F} \;=\; G\dot{\Phi}^2 \tag{2.6}$$

This is the mesoscopic version of Joule law. The expression for the conductance is

$$G = \mathsf{g}(E_F) \times \frac{1}{2}\int_{-\infty}^\infty C(\tau)d\tau \tag{2.7}$$

2.1   The Kubo formula

The above is apparently the simplest and most illuminating derivation of the Fluctuation-Dissipation version of the Kubo formula. A more complicated treatment [28, 30, 31] allows to write a generalized version Namely,

$$G = \mathsf{g}(E_F) \times \int_0^\infty C(\tau)d\tau \tag{2.8}$$

with

$$C(\tau) = \langle \mathcal{I}(\tau)\mathcal{F}(0)\rangle_E \tag{2.9}$$

where $\mathcal{F}$ is the generalized force which is associated with the driving. In the present application $\mathcal{F}$ is just the current operator, hence $C(\tau)$ is symmetric, and therefore the generalized version Eq.(2.8) is equivalent to Eq.(2.7).

It is also important to make a connection with the more traditional treatment of conductance in case of disordered metals. If we set $a(x) = 1/L$ for the vector potential we get $(e/L)\hat{v}$ as the current operator. Hence we get from Eq.(2.7)

$$G = \mathsf{g}(E_F) \times \frac{1}{2}\left(\frac{e}{L}\right)^2 \int_{-\infty}^\infty \langle v(\tau)v(0)\rangle d\tau \tag{2.10}$$

The conventional derivation of the Drude formula is based on the assumption of exponential decay of the velocity-velocity correlation function. The latter formula is (formally) valid in any case, but in case of a disordered sample it has special appeal because it implies the Einstein relation between the conductance and the spatial diffusion. Namely, if we have a diffusive ring then it is natural to write $G = \hat{G}/L$ and to define $\hat{\mathbf{g}}(E_F) = \mathbf{g}(E_F)/L$. Then we can rewrite Eq.(2.10) as

$$\hat{G} = e^2 \hat{\mathbf{g}}(E_F) D_{\text{space}} \tag{2.11}$$

The more conventional derivations of this expression is based on the phenomenological relation $J = -D\nabla(\text{density}) - \hat{G}\nabla(\text{potential})$ and the argument that $J = 0$ at equilibrium.

The "classical" Kubo formula implies in this context that the current-current correlation function is evaluated classically, ignoring quantum interference. In the case of hard chaos system this correlation function decays exponentially. The Drude expression is the simplest classical approximation:

$$\langle \mathcal{I}(\tau)\mathcal{I}(0) \rangle = \frac{1}{d}\left(\frac{e}{L}v_{\text{F}}\right)^2 \exp\left[-2\left(\frac{v_{\text{F}}}{\ell}\right)\tau\right] \tag{2.12}$$

Substitution into the Kubo formula leads to

$$G_{\text{Drude}} = \frac{e^2}{2\pi\hbar}\mathcal{M}\frac{\ell}{L} \tag{2.13}$$

where we have dropped the d dependent prefactor which equals 1 for networks ($d = 1$). In the case of a ballistic ring with a restricted scattering region (as in Fig. 1d) it is more convenient to characterize the device by its total transmission $0 < g_T < 1$ instead of the mean free path. The envelope of the current-current correlation function is

$$|2g_T - 1|^{\#\text{rounds}} \quad \Leftrightarrow \quad \exp\left[-2\left(\frac{v_{\text{F}}}{\ell}\right)|\tau|\right] \tag{2.14}$$

With the identification of #rounds as $t/(L/v_{\text{F}})$ we deduce that for $g_T \sim 1$ the mean free path is $\ell \approx L/(1 - g_T)$.

2.2 Implications of the Kubo formula

From the Kubo formula Eq.(2.8) it is not obvious that the result for G is independent of where we measure $\mathcal{I}$. In general it can be proved [32] that for a different choice of $\mathcal{I}$ the corresponding Kubo conductance may differ at most by $e\mathsf{g}(E_F)\langle\mathcal{F}\rangle$. But if $\mathcal{F}$ is a current operator then $\langle\mathcal{F}\rangle = 0$ and therefore the conductance becomes independent of x_1.

Also it seems that the Kubo conductance is proportional to the density of states. Therefore, if we had doubled the volume of the cavity, would we get larger conductance? Furthermore, does the result for G depends merely on the transition matrix, and not (say) on the dwell time inside the scattering region?

To answer these questions, and to establish the x_1 independence of G, let us write the Kubo formula in a more illuminating way. By definition we have

$$\int_{-\infty}^{\infty}\langle\mathcal{I}(\tau)\mathcal{F}(0)\rangle d\tau = \sum_r p_r\mathcal{F}_rQ_r$$

$$\equiv \frac{1}{\mathsf{g}(E)}\int \delta(E-\mathcal{H}(\boldsymbol{r},\boldsymbol{p}))\frac{d\boldsymbol{r}d\boldsymbol{p}}{(2\pi)^d}F(\boldsymbol{r},\boldsymbol{p})Q(\boldsymbol{r},\boldsymbol{p}) \tag{2.15}$$

where r is an index that labels phase space cells (different initial conditions), and p_r corresponds to a microcanonical distribution. We have introduced the notation

$$Q(\boldsymbol{r},\boldsymbol{p}) = \int_{-\infty}^{\infty}\mathcal{I}(\tau;\boldsymbol{r},\boldsymbol{p})d\tau \tag{2.16}$$

Namely $Q(\boldsymbol{r},\boldsymbol{p})$ is the total charge which is obtained by integrating the current which is induced by a particle that goes through the point $(\boldsymbol{r},\boldsymbol{p})$ at $t = 0$. It is in fact (for $e = 1$) the winding number of the associated trajectory, and therefore it gives a result which is independent of the chosen section. Note however that $Q(\boldsymbol{r},\boldsymbol{p})$ obtains a meaningful value only upon course graining, else it is erratic. Now we can write the Kubo formula as

$$G = \frac{1}{2}\int \delta(E-\mathcal{H}(\boldsymbol{r},\boldsymbol{p}))\frac{d\boldsymbol{r}d\boldsymbol{p}}{(2\pi)^d}F(\boldsymbol{r},\boldsymbol{p})Q(\boldsymbol{r},\boldsymbol{p}) \tag{2.17}$$

This expression has several advantages. One advantage we have mentioned: the result is manifestly independent of the definition of the current operator. The second advantage is

that it shows that the global density of states is in fact not important. We can double the volume of the cavity, still we would get the same result provided that the scattering probabilities are not affected. In particular we see that time delays are not important.

2.3   The quantum Kubo formula and beyond

In this section our objective is to find the conductance of the closed ring in circumstances such that the motion inside the ring is coherent (quantum interference within the bonds is not ignored). The calculation is done using the quantum version of Eq.(2.8) which involves the matrix elements $\mathcal{I}_{nm}$ of the current operator:

$$G = \pi\hbar \; \varrho_{\mathrm{F}}^2 \times \langle\langle|\mathcal{I}_{nm}|^2\rangle\rangle \tag{2.18}$$

This equation would be the traditional Kubo formula if $\langle\langle...\rangle\rangle$ stood for a simple algebraic average over near diagonal matrix elements at the energy range of interest. By near diagonal elements we mean $|E_n - E_m| \lesssim \Gamma$, where Γ is level broadening parameter. The levels of the system are effectively "broadened" due to the non-adiabaticity of the driving [33] or due to the interaction with the noisy environment [6]. In what follows we assume

$$\Delta \;\ll\; \Gamma \;\ll\; \Delta_b \tag{2.19}$$

where $\Delta = 1/\varrho_{\mathrm{F}}$ is the mean level spacing, and $\Delta_b = \pi\hbar v_{\mathrm{F}}/L$ is the Thouless energy. (Note that $\Delta_b/\Delta = \mathcal{M}$). Contrary to the naive expectation it has been argued in [11] that depending on the physical circumstances the definition of $\langle\langle...\rangle\rangle$ may involve a more complicated *coarse graining* procedure. Consequently the result for G may differ by orders of magnitude from the traditional Kubo-Drude result. We shall discuss this key observation in later sections.

For a network system $\varrho_{\mathrm{F}} = \mathcal{M}L/(\pi\hbar v_{\mathrm{F}})$. Furthermore it is convenient to define a scaled matrix I_{nm} via the relation

$$\mathcal{I}_{nm} = -i(ev_{\mathrm{F}}/L)I_{nm} \tag{2.20}$$

so as to deal with real dimensionless quantities. Thus we re-write Eq.(2.18) as:

$$G = \frac{e^2}{2\pi\hbar} \, 2\mathcal{M}^2 \, \mathbf{g} \qquad (2.21)$$

where $\mathbf{g} \equiv \langle\langle|I_{nm}|^2\rangle\rangle$. In later sections we shall discuss the recipe for the $\mathbf{g}$ calculation. It is important to realize (see section 4.2) that $\mathbf{g} < 1$. This implies a quantum mechanical bound on G.

Chapter 3

The classical conductance for a multi-mode ring

3.1 Setting up the model

Consider non-interacting spinless electrons in a ring, as in Fig.1b. The one-particle Hamiltonian is

$$\mathcal{H} = \frac{1}{\mathsf{m}}(\boldsymbol{p} - e\Phi a(\boldsymbol{r}))^2 + V(\boldsymbol{r}) \tag{3.1}$$

where m and e are the mass and the charge respectively. The vector potential which is associated with the flux Φ is described by

$$\oint a(\boldsymbol{r}) \cdot d\boldsymbol{r} = 1 \tag{3.2}$$

The dimensionality of the ring is d. The ring consists of a "wire" region and a scattering region. The motion of the particle inside the ring is assumed to be globally chaotic. The coordinate along the wire will be denoted as x. The scattering region is located at $x \sim 0$.

In the geometry of Fig.1b the "wire" is a $d = 2$ waveguide of width W. Later we describe the waveguide as a set of $d = 1$ wires (Fig.1d) such that each "wire" corresponds to

an open mode of the waveguide. The length of the ring L is assumed to be large compared with the scattering region so as to allow meaningful definition of a scattering matrix in the quantum mechanical analysis (evanescent modes are ignored).

The ring is driven by a time dependent Aharonov-Bohm flux. The EMF $-\dot{\Phi}$ is assumed to be constant. There are various ways to introduce the EMF into the ring. One possibility is to have all the voltage drop over a section at $x = x_0$. Namely,

$$a(x) = \delta(x - x_0) \tag{3.3}$$

For sake of later analysis we define a generalized force which is associated with the flux:

$$\mathcal{F} = -\frac{\partial \mathcal{H}}{\partial \Phi} = e\hat{v}\delta(\hat{x} - x_0) \tag{3.4}$$

where v is the velocity in the x direction. In the quantum mechanical case a symmetrization is implicit. This is in fact a current operator. Obviously we do not have to measure the current at the same point where we apply the voltage. So for sake of generality we introduce the notation

$$\mathcal{I} = e\hat{v}\delta(\hat{x} - x_1) \tag{3.5}$$

We also note that with uniform averaging over x_1 we get $(e/L)\hat{v}$ which is essentially the velocity operator.

In the absence of driving the "pure" stationary states of the system are the microcanonical states. We use classical language but also have in mind a semiclassical picture. Each microcanonical state occupy a shell whose phase space volume is $(2\pi\hbar)^d$. The density of states is

$$\mathsf{g}(E) = \int \int \frac{d\mathbf{r}d\mathbf{p}}{(2\pi\hbar)^d} \delta(E - \mathcal{H}(\mathbf{r}, \mathbf{p})) \tag{3.6}$$

The zero order stationary state is characterized by an occupation function $f(E)$. Later we shall take it to be the Fermi function. Thus

$$dN = \rho(\mathbf{r}, \mathbf{p}) \frac{d\mathbf{r}d\mathbf{p}}{(2\pi\hbar)^d} = f(E) \frac{d\mathbf{r}d\mathbf{p}}{(2\pi\hbar)^d} \tag{3.7}$$

29

where $E = H(\boldsymbol{r}, \boldsymbol{p})$ is the energy. The distribution of the particles in energy is

$$\rho(E) = \mathsf{g}(E)f(E) \tag{3.8}$$

and the total number of particles is

$$N = \int \int \rho(\mathbf{r}, \mathbf{p}) \frac{d\mathbf{r}d\mathbf{p}}{(2\pi\hbar)^d} = \int_{-\infty}^{\infty} \rho(E)dE = \int_{-\infty}^{\infty} f(E)\mathsf{g}(E)dE \tag{3.9}$$

3.2 Network modeling

A network is defined as a set of 1D wires that are connected in vertices. The network Hamiltonian is ill defined in the classical limit because the the scattering in each vertex is described by a scattering matrix. In particular for the model of Fig.1d the scattering is described by a scattering matrix S_{ab}, and we define the corresponding transition matrix as $g_{ab} = |S_{ab}|^2$. Thus the classical description of the system is stochastic rather than deterministic.

Still we can regard networks as an effective way to describe the chaotic dynamics [34]. The reason is that upon coarse graining a chaotic system looks like a stochastic model. Specifically, in the case of the system of Fig1b, quantum mechanics introduces "coarse graining" in a most natural way. Each mode in the scattering problem can be regarded as a 1D wire with the dispersion relation

$$v_n = \frac{1}{\mathsf{m}} \sqrt{2\mathsf{m}E - \left(\frac{\pi\hbar}{W}n\right)^2} \tag{3.10}$$

where E is the energy of the particle, and W is the width of the waveguide. The open modes are those for which v_n is a real number. We shall denote the number of open modes by $\mathcal{M}$ hence the number of open channels in the open geometry is $2\mathcal{M}$.

The density of states of the system can be written as a sum over single-mode expressions:

$$\mathsf{g}(E) = \mathsf{g}_{\text{dot}}(E) + 2\sum_{n=1}^{\mathcal{M}} \frac{L}{(2\pi\hbar)} \frac{1}{v_n(E)} \tag{3.11}$$

where the factor of two takes into account both clockwise and anticlockwise motion. A stationary state of the system is described by the distribution functions $\rho_n^{\rightarrow}(E)$ of the clockwise moving particles and $\rho_n^{\leftarrow}(E)$ of the counter-clockwise moving particles. The index n distinguishes different modes. The normalization is such that

$$N = \int \rho_{\text{dot}}(E) dE + L \sum_n \int (\rho_n^{\rightarrow}(E) + \rho_n^{\leftarrow}(E)) dE \tag{3.12}$$

The density of particles per unit length in a given mode is implied by Eq.(3.8):

$$\rho_n^{\rightarrow}(E) dE = \rho_n^{\leftarrow}(E) dE = \frac{dE}{(2\pi\hbar) v_n(E)} f(E) \tag{3.13}$$

Note that for a microcanonical distribution dE can be regarded as a fixed parameter that defines an energy window or a width of an energy shell.

The scattering is described by a $2\mathcal{M} \times 2\mathcal{M}$ transition matrix that has a block structure:

$$g_{ab} = \begin{pmatrix} g^R & g^T \\ g^T & g^R \end{pmatrix} \tag{3.14}$$

It consists of the reflection matrix g_{nm}^R and the transmission matrix g_{nm}^T. Note that the channel index a contains both mode specification and left/right lead specification. We assume time reversal invariance, so as to have a symmetric matrix. For clarification we note that if N particles incident in channel b, then $g_{ab}N$ particles emerge in channel a. This means that g_{ab} is the ratio between ingoing and outgoing fluxes. In the ergodic state Eq.(3.13) implies that $\rho_a \propto 1/v_a$. Therefore we have detailed balance:

$$g_{ab}\, \rho_b v_b \;=\; g_{ba}\, \rho_a v_a \qquad \text{[no summation]} \tag{3.15}$$

Namely, for a stationary state the transitions from a to b are exactly balanced by the transitions from b to a.

3.3   Conductance of a single mode ring (part 1)

In this section we show how the Kubo formula for a *closed* ring leads to a Landauer-alike formula for the conductance provided the effect of the environment is to completely random-

ize the velocity within the wire region without affecting its transmission. To simplify the presentation we consider the single mode case.

For the Kubo formula we have to evaluate the correlation function $C(\tau)$ of Eq.(2.9), and to calculate the integral in Eq.(2.8). As explained the result of the calculation should be independent of the how we define the current operators. The simplest choice is to define $\mathcal{F}$ as the current through a section $x = x_0$ on the left of the scattering region, while $\mathcal{I}$ is the current through a section $x = x_1$ on the right of the scattering region. $C(\tau)$ comes out as a sum of delta functions. The shortest time correlation is associated with the time τ_1 to cross the scattering region. For example, if there is no time delay then $\tau_1 = (x_1 - x_0)/v_E$. We can regularize $\mathcal{F}$ as a rectangular of width ε. The probability to have there a particle moving in the right direction, such that $\mathcal{F}(0) = ev_E/\varepsilon$ is $(\varepsilon/L)/2$. The current that we get in the other side of the barrier is $\mathcal{I} = e\delta(\tau - \tau_1)$. Assuming that this is the only correlation, and taking into account the time reversed correlation for $\tau < 0$, we get

$$C(\tau) = e^2 \frac{v_{\mathrm{F}}}{L} \sum_{\pm} \frac{1}{2} g_T \delta(\tau \mp \tau_1) \tag{3.16}$$

Note that if we had chosen $x_1 = x_0$ we would get three delta functions: a self correlation delta function $\delta(\tau)$ and reflection peaks. Namely,

$$C(\tau) = e^2 \frac{v_{\mathrm{F}}}{L} \left[\delta(\tau) - \frac{1}{2}(1 - g_T) \sum_{\pm} \delta(\tau \mp \tau_0) \right] \tag{3.17}$$

where τ_0 is the scattering time. Obviously the integral over the new $C(\tau)$ is the same as the integral over the former one. Irrespective of our choices we get from Kubo

$$\boldsymbol{G} = \frac{e^2}{2\pi\hbar} g_T \tag{3.18}$$

which looks like the (single mode) Landauer formula.

3.4 Conductance of a single mode ring (part 2)

If the velocity is not randomized within the wire, then there are other correlations that involve the time L/v_E to encircle the ring. For the following calculation it is simplest to assume that $0 < x_0 < x_1$. What we have is to calculate the integral

$$\int_0^\infty \langle \mathcal{I}(\tau)\mathcal{F}(0)\rangle d\tau = \sum_r p_r \mathcal{F}_r Q_r \tag{3.19}$$

Note that we find it convenient here to set $\tau = 0$ as the lower bound of the integral. Recall that r is an index that labels phase space cells (different initial conditions), and p_r corresponds to a microcanonical distribution. Note that $\mathcal{F}$ is non-zero only if r is located at $x = x_0$. The total charge which is transported through the section $x = x_1$ is defined here as

$$Q_r = \int_0^\infty \langle \mathcal{I}(\tau)\rangle_r d\tau \tag{3.20}$$

where the current is evaluated under the assumption that the particle is launched at point r. There are two relevant possibilities: Either the particle is launched at $x = x_0$ in the clockwise direction, or it is launched at $x = x_0$ in the anti-clockwise direction. Observe that the (net) charge that goes through the section $x = x_1$ after a round trip is suppressed by a factor $(2g_T - 1)$ due to the scattering (we sum the clockwise and the anticlockwise contributions). Thus we get that the total charge that goes through the section is

$$Q^\rightarrow = e\left[1 + (2g_T - 1) + (2g_T - 1)^2 + ...\right] = e\left[\frac{1}{2(1 - g_T)}\right] \tag{3.21}$$

for a particle that is launched clockwise, and

$$Q^\leftarrow = -e\left[\frac{1}{2(1 - g_T)} - 1\right] \tag{3.22}$$

for a particle that is launched anti-clockwise Thus we get

$$\int_0^\infty \langle \mathcal{I}(\tau)\mathcal{F}(0)\rangle d\tau = \frac{1}{2L}(+ev_E)Q^\rightarrow + \frac{1}{2L}(-ev_E)Q^\leftarrow = e^2\frac{v_E}{L}\left[\frac{g_T}{1 - g_T}\right] \tag{3.23}$$

leading to

$$G = \frac{e^2}{2\pi\hbar}\left[\frac{g_T}{1 - g_T}\right] \tag{3.24}$$

33

3.5 Relation to the Landauer formula

As explained in section 3.3 we get from the Kubo formula a Landauer look-alike formula if we assume that the environment induces velocity randomization in the wire region without affecting its transmission. In fact we can get to the same conclusion by modeling the "loss of memory" in the wire region as a scatterer with transmission $g_{\text{wire}} = 1/2$. It is well know that the G of Eq.(3.24) obeys Ohm law for addition of resistors in series. Hence

$$\boldsymbol{G} = \frac{e^2}{2\pi\hbar} \left(\frac{g_T}{1 - g_T} \right) = \frac{e^2}{2\pi\hbar} \left[\left(\frac{g_0}{1 - g_0} \right)^{-1} + \left(\frac{g_{\text{wire}}}{1 - g_{\text{wire}}} \right)^{-1} \right]^{-1} = \frac{e^2}{2\pi\hbar} g_0 \qquad (3.25)$$

We would like to emphasize that the purpose of this section is purely pedagogical. As stated in section 1.3 an environment that just randomize the velocity without affecting the transmission is apparently of no physical interest. Still if one insists it can be constructed artificially. Simply cut the wire and connect the two ends to a chaotic cavity. A particle that moves in the wire gets into the cavity and after a time delay gets out either clockwise or anti-clockwise with equal probabilities. Hence in such arrangement $g_{\text{wire}} = 1/2$.

The pedagogical importance of the above discussion is in making a bridge between the reservoir philosophy of the Landauer construction and the Kubo formalism of closed systems. The memory loss device that we have described above provides the same "service" as the reservoirs in the Landauer picture.

3.6 Conductance of a multi-mode ring

Let us assume that the EMF $-\dot{\Phi}$ is concentrated across the scattering region ($x_0 = 0$). When a particle goes through $x = 0$ it gains momentum ($p \mapsto p - e\dot{\Phi}/v$), where $v = |p|/\mathsf{m}$. Hence the change is energy is $E \mapsto E \mp e\dot{\Phi}$ for right and left movers respectively. The state of the system is described by the distribution functions $\rho_n^{\rightarrow}(E)$ and $\rho_n^{\leftarrow}(E)$ of Eq.(3.12). The index n distinguishes different modes. It is implicit from now on that we look for an ergodic-

like solution, such that the density of the particles along the ring is uniform. The balance equations are:

$$\frac{\partial \rho_n^{\rightarrow}}{\partial t} = -[\rho_n^{\rightarrow} v_n] + \left[\sum_m g_{nm}^T \rho_m^{\rightarrow} v_m\right]_{E+e\dot{\Phi}} + \left[\sum_m g_{nm}^R \rho_m^{\leftarrow} v_m\right] \tag{3.26}$$

$$\frac{\partial \rho_n^{\leftarrow}}{\partial t} = -[\rho_n^{\leftarrow} v_n] + \left[\sum_m g_{nm}^T \rho_m^{\leftarrow} v_m\right]_{E-e\dot{\Phi}} + \left[\sum_m g_{nm}^R \rho_m^{\rightarrow} v_m\right] \tag{3.27}$$

It can be verified that the zero order ($\dot{\Phi} = 0$) stationary solution of this equation is given by Eq.(3.13), where $f(E)$ is an arbitrary function. We are looking for a first order stationary-like solution. The linearized equation for the clockwise moving particles is

$$\left[\sum_m (1 - g^T)_{nm} \delta \rho_m^{\rightarrow} v_m\right] - \left[\sum_m g_{nm}^R \delta \rho_m^{\leftarrow} v_m\right] = \frac{e}{2\pi} \dot{\Phi} \frac{\partial f(E)}{\partial E} \sum_m g_{nm}^T \tag{3.28}$$

A similar equation exist for the counter-clockwise particles. Subtracting the corresponding equations we get

$$\sum_m [(1 - g^T) + g^R]_{nm} [\rho^{\rightarrow} v - \rho^{\leftarrow} v]_m = 2 \frac{e}{2\pi} \dot{\Phi} \frac{\partial f(E)}{\partial E} g_n \tag{3.29}$$

with the solution

$$[\rho^{\rightarrow} v - \rho^{\leftarrow} v]_n = \frac{e}{2\pi} \dot{\Phi} \frac{\partial f(E)}{\partial E} \sum_{n'} \left[\frac{2}{(1 - g^T) + g^R}\right]_{nn'} g_{n'} \tag{3.30}$$

The current is

$$\begin{aligned}
\mathcal{I} &= \sum_n \int_0^{\infty} dE \, (\rho_n^{\rightarrow} - \rho_n^{\leftarrow}) e v_n \\
&= \dot{\Phi} \frac{e^2}{2\pi} \int_0^{\infty} \sum_{nm} \left[\left(\frac{2}{1 - g^T + g^R}\right) g^T\right]_{nm} \frac{\partial f(E)}{\partial E} dE
\end{aligned} \tag{3.31}$$

With the assumption of Fermi occupation we get Eq.(1.11). Note that upon summation the order of matrix multiplication is not important because g_{nm} is symmetric.

35

3.7 The wire with cavity model system

We consider a ring (Fig.1b) which is formed by folding a rectangular waveguide (i.e. imposing periodic boundary conditions). A chaotic cavity is attached to the waveguide at one "point". A particle has some probability to enter the cavity, where memory is "lost", and then it gets out again with equal probability to either side. A particle that travels in mode n of the waveguide has a transverse momentum $\pm(\pi\hbar/W)n$ where W is the width of the waveguide. The distance between subsequent hits of the same wall is

$$\text{step} = \frac{\sqrt{2\mathsf{m}E - ((\pi\hbar/W)n)^2}}{(\pi\hbar/W)n} 2W = \frac{\sqrt{\mathcal{M}^2 - n^2}}{n} 2W \tag{3.32}$$

The number of open modes $\mathcal{M}$ is implicitly defined via the latter equality. The probability to get into the cavity via an opening of size L_{op} is:

$$p_n = \frac{L_{\text{op}}}{\text{step}} = \text{minimum}\left[\frac{\alpha}{\sqrt{(\mathcal{M}/n)^2 - 1}},\ 1\right] \tag{3.33}$$

where $\alpha = L_{\text{op}}/(2W)$. The crossover from $p_n < 1$ to $p_n = 1$ happens at

$$n_c = \frac{1}{\sqrt{1+\alpha^2}}\mathcal{M} \tag{3.34}$$

We are going to treat $\mathcal{M}$ as a free parameter. Hence we have two parameters that characterize the scattering: the classical (geometrical) parameter α, and the quantum-mechanical parameter $\mathcal{M}$. Note that the classical limit is $\mathcal{M} \to \infty$.

Let q_n be the probability to get out of the box to mode n, either to the right going channel or to the left going channel. It follows that $g_{nm}^R = (1/2)q_n p_m$. From $g_{nm} = g_{mn}$ we conclude that $q_n/p_n = c$ is the same for all channels. Taking into account that $\sum_n q_n = 1$ we get $c = 1/(\sum_n p_n)$, and hence

$$g_{nm}^R = \frac{1}{2}q_n p_m = \frac{c}{2}p_n p_m \tag{3.35}$$

$$g_{nm}^T = \frac{1}{2}q_n p_m + (1 - p_m)\delta_{nm} = \frac{c}{2}p_n p_m + (1 - p_m)\delta_{nm} \tag{3.36}$$

Thus, given the input parameters α and $\mathcal{M}$, we can calculate g_{nm}. It is useful to define the total probability of transmission for a particle that comes in channel n as:

$$g_n \equiv \sum_m g_{mn}^T = 1 - \frac{1}{2} p_n \tag{3.37}$$

For sake of later estimates we note that for $\mathcal{M} \gg 1$, sums over n can be approximated by an integral over $x = n/\mathcal{M}$. Using the obvious notation $x_c = n_c/\mathcal{M}$ we get

$$
\begin{aligned}
\frac{1}{\mathcal{M}} \sum p_n &\approx \alpha \int_0^{x_c} [(1/x)^2 - 1]^{-1/2} dx + [1 - x_c] \\
&= \alpha \frac{1}{2} \left[1 - (1 - x_c^2)^{1/2} \right] + [1 - x_c] \\
&= 1 + \frac{1}{2} \alpha - (1 + \alpha^2)^{-1/2} \left(1 + \frac{1}{2} \alpha^2 \right) \\
&\approx \frac{1}{2} \alpha + \mathcal{O}(\alpha^4)
\end{aligned}
\tag{3.38}
$$

and

$$
\begin{aligned}
\frac{1}{\mathcal{M}} \sum \frac{1}{p_n} &\approx \frac{1}{\alpha} \int_{1/\mathcal{M}}^{x_c} [(1/x)^2 - 1]^{1/2} dx + [1 - x_c] \\
&= \frac{1}{\alpha} \left[\ln \left(\frac{2x_c}{1 + (1 - x_c^2)^{1/2}} \mathcal{M} \right) - \left(1 - (1 - x_c^2)^{1/2} \right) \right] + [1 - x_c] \\
&= \frac{1}{\alpha} \left[\ln \left(\frac{2}{\alpha + (1 + \alpha^2)^{1/2}} \mathcal{M} \right) - 1 \right] + 1 \\
&\approx [\ln(2\mathcal{M}) - 1] \frac{1}{\alpha} + \mathcal{O}(\alpha)
\end{aligned}
\tag{3.39}
$$

We now turn to the calculation of the conductance. First of all, let us calculate the Landauer conductance. Thanks to the simple structure of the g_{nm}^T matrix, the calculation is quite easy

$$G_{\mathrm{Landauer}} = \frac{e^2}{2\pi\hbar} \sum_{n,m} g_{nm}^T = \frac{e^2}{2\pi\hbar} \sum_n g_n \tag{3.40}$$

37

Each channel has total transmission in the range $(1/2) < g_n < 1$ and therefore the conductance (in normalized units) roughly equals to the number of open modes. Substitution of (3.37) leads to:

$$G_{\text{Landauer}} = \frac{e^2}{2\pi\hbar} \sum_n (1 - (p_n/2)) = \frac{e^2}{2\pi\hbar} [1 - \frac{1}{4}\alpha + \mathcal{O}(\alpha^4)]\mathcal{M} \tag{3.41}$$

For the multimode conductance of Eq.(1.11) the calculation is more complicated. At first sight it seems that the calculation should be done numerically as in Fig. 4. The numerical calculation in Fig. 4 (circles) is done in a way which is inspired by a similar type of calculation within the Landauer formalism. We define $h_{nm} = ([2g^T/(1 - g^T + g^R)]_{nm})^{1/2}$ and write the sum in Eq.(1.11) as trace $[h^\dagger h]$. Then we make singular value decomposition of h and sum over the squares of its eigenvalues.

The other way to calculate the multimode conductance starts with an attempt to make a zero order evaluation of the sum. This means setting $c = 0$ in Eq.(3.36). The resulting estimate gives a rough approximation as seen from Fig.4 (crosses). The main source of error are evidently the low modes. Surprisingly it turns out that the calculation can be carried out to infinite order in c, thanks to miraculous cancellations. Using the expansion

$$\frac{1}{A - cB} = \frac{1}{A} + c\frac{1}{A}B\frac{1}{A} + c^2\frac{1}{A}B\frac{1}{A}B\frac{1}{A} + \dots \tag{3.42}$$

with $A_{nm} = p_n\delta_{nm}$ and $B_{nm} = (1/2)p_np_m$, we get the result

$$\begin{aligned}
\left[\frac{1}{1 - g^T}\right]_{nm} &= \frac{1}{p_n}\delta_{nm} + (c/2)\frac{1}{p_n}p_np_m\frac{1}{p_m} + \\
&+ (c/2)^2\sum_k \frac{1}{p_n}p_np_k\frac{1}{p_k}p_kp_m\frac{1}{p_m} + \dots = \frac{1}{p_n}\delta_{nm} + c
\end{aligned} \tag{3.43}$$

where in the last step we have made a geometric summation over all orders. Now we can calculate the conductance

$$G = \frac{e^2}{2\pi\hbar} \sum_{n,m} \left[\frac{g^T}{1 - g_T}\right]_{nm} = \frac{e^2}{2\pi\hbar}\left[\left(\sum_n \frac{1}{p_n}\right) + c\mathcal{M}^2 - \mathcal{M}\right] \tag{3.44}$$

38

Recall that $c = 1/\sum_n p_n$. Hence this expression requires merely the evaluation of the sums $\sum_n p_n$ and $\sum_n(1/p_n)$. If we have $p_n \approx 1$ for all modes, then we get simply $G = (e^2/(2\pi\hbar))\mathcal{M}$ which reflects that number of open modes. But the interesting case is when α is small:

$$G \approx \frac{e^2}{2\pi\hbar}\left[\frac{1}{\alpha}(1 + \ln(2\mathcal{M})) - 1 + \mathcal{O}(\alpha)\right]\mathcal{M} \tag{3.45}$$

Unlike the case of the Landauer conductance, the result does not reflect the number of open modes. The contribution of the low modes is singular in the limit of small α. Furthermore, the conductivity (conductance per channel) diverges logarithmically in the classical limit.
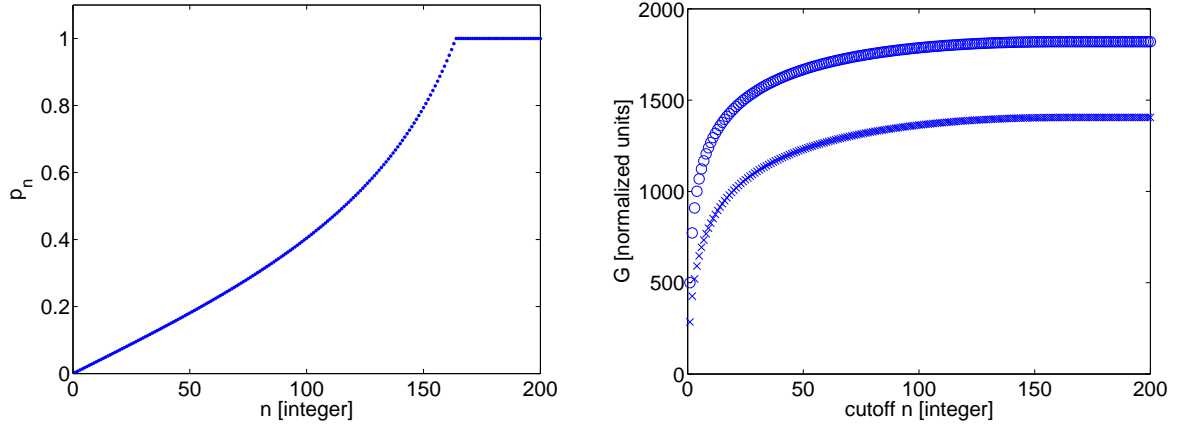

Fig.4 The left panel displays p_n for a system with $\alpha = 0.7$ and $\mathcal{M} = 200$ open modes. The crosses in the right panel are for the cumulative sum over $(1 - p_n)/p_n$. The circles are calculated from the exact formula. Namely, the matrix h is diagonalized, and the cumulative trace over the square of its elements is displayed.

Chapter 4

The conductance of multimode ballistic rings

4.1 Model for ballistic rings

We now turn to consider the case of a coherent ring, a simple model for a ballistic ring can be either of the "disordered type" or of the "chaotic type". Let us visualize the disordered potential as arising from a set of scatterers which are distributed all over the ring (Fig 5a). Depending on the scattering cross section of the individual scatterers we can have $\ell \ll L$ for strong disorder or $\ell \gg L$ for weak disorder, where ℓ is the mean free path for velocity randomization, and L is the perimeter of the ring.

Another possibility is not to make all the scatterers smaller, but rather to dilute them. Eventually we may have a chaotic ring where the scattering is induced by a single scatterer (Fig 5b). For example the scatterer can be a disc or a semi-disc as in Fig 6. These variations of Sinai billiard (billiard with convex wall elements) are known to be chaotic. It is important to remember that "chaos" means that complicated ergodic classical dynamic is generated by a simple Hamiltonian (*no disorder!*).

In our view chaotic rings are more interesting for various reasons. Ballistic devices are state-of-art in mesoscopic experiments. For example it is quite common to fabricate Aharonov-Bohm devices. In such devices it is possible to induce local deformation of the potential by means of a gate voltage. Hence one has a full control over the amount of scattering. Also from theoretical point of view it is nice to have a well defined scattering region: This allows to use the powerful S-matrix point of view that has been initiated by Landauer. In particular we can ask what is the conductance of a device depending on whether it is integrated in an open geometry as in Fig. 5e or in a closed geometry as in Fig. 5d. We believe that "chaos" and "disorder" lead to similar physics in the present context, but this claim goes beyond the scope of the present work.

A multimode ring can be visualized as a waveguide of length L and width W. In such case the number of open modes is $\mathcal{M} \propto (k_{\mathrm{F}}W)^{d-1}$ where $d = 2, 3$ is the dimensionality. We label the modes as

$$a \quad = \quad \text{mode index} \quad = \quad 1, 2, ..., \mathcal{M} \tag{4.1}$$

The scattering arise due to some bump or some deformation of the boundary, and can be described by an $2\mathcal{M} \times 2\mathcal{M}$ scattering matrix $\boldsymbol{S}$. For the semi-disc model analytical complicated expressions are available [35, 36]. The "classical" transitions probability matrix $\boldsymbol{g}$ is obtained by squaring the absolute values of the $\boldsymbol{S}$ matrix elements.

Disregarding the closed channels, the ballistic ring is described as a set of $\mathcal{M}$ open modes, and a small scattering region that is characterized by its total transmission g_T. Optionally the ballistic ring can be regarded as a network: Each bond corresponds to an open mode. Let us consider the simplest model where the scattering is the same for an incident particle that comes from the left or from the right:

$$\boldsymbol{g} = \begin{pmatrix} [\boldsymbol{g}^R]_{a,b} & [\boldsymbol{g}^T]_{a,b} \\ [\boldsymbol{g}^T]_{a,b} & [\boldsymbol{g}^R]_{a,b} \end{pmatrix} \tag{4.2}$$

where $\boldsymbol{g}^R$ is the reflection matrix and $\boldsymbol{g}^T$ is the transmission matrix. The simplest model

that one can imagine is with

$$[\boldsymbol{g}^R]_{a,b} \;=\; \epsilon^2 \tag{4.3}$$

$$[\boldsymbol{g}^T]_{a,b} \;=\; (1 - \mathcal{M}\epsilon^2)\delta_{a,b} \tag{4.4}$$

such that the total transmission is

$$g_T = 1 - \mathcal{M}\epsilon^2 \tag{4.5}$$

Such "classical" transitions probability matrix can arise if we take the S matrix as

$$\boldsymbol{S}_{\mathrm{D}} = \begin{pmatrix} \epsilon \exp\left(i\,2\pi\,\frac{a\,b}{\mathcal{M}}\right) & \sqrt{1 - \mathcal{M}\epsilon^2}\,\delta_{a,b} \\[2mm] \sqrt{1 - \mathcal{M}\epsilon^2}\,\delta_{a,b} & -\epsilon\exp\left(-i\,2\pi\,\frac{a\,b}{\mathcal{M}}\right) \end{pmatrix} \tag{4.6}$$

There a lot of simplifications that were involved in construction this $\boldsymbol{S}$ matrix.

- The forward scattering is to the same mode only

- The back scattering is "isotropic"

- The scattering is energy independent

- The scattering phases are not random

One can wonder whether this $\boldsymbol{S}$ matrix still qualifies as 'generic', or maybe the model is over-simplistic. In order to illuminate this point let us look at the Sinai billiard models of Fig. 6. These models are fully qualified as "quantum chaos" systems. One observes that the specific $\boldsymbol{g}$ matrix of Eq.(4.3-4.4) is inspired by that of Fig. 6a. In this billiard an incident particle is equally likely to be scattered to any mode in the backward direction, but the forward scattering is only to the same mode (same angle). As for the phases: we already have explained that our interest is not in disordered ring, but rather in chaotic one. Therefore to have random phases in the $\boldsymbol{S}$ matrix is not an essential feature of the model. The phases are effectively randomized simply because the wavenumber k_a is different in each

mode. Optionally, it is more convenient to assume that all the k_a are the same, and to have instead bonds with different lengths L_a. This provides the required phase randomization.

Let us see what do we get for G_{Landauer} and for G_{Drude} in the case of the prototype system that we have defined. The calculation of G_{Landauer} is trivial and leads to Eq.(1.14). The calculation of G_{Drude} is more complicated since it involves matrix inversion. Still $\boldsymbol{g}$ is sufficiently simple to allow a straightforward calculation that leads to Eq.(1.15). The rest of this section is devoted to the details of this calculation.

We write $\boldsymbol{g}_T = \tau^2 \mathbf{1}$ and $\boldsymbol{g}_R = \epsilon^2 \boldsymbol{\Upsilon}$, where τ and ϵ are defined via $g_T = \tau^2 = 1 - \mathcal{M}\epsilon^2$, and where we have introduced the following $\mathcal{M} \times \mathcal{M}$ matrices

$$\mathbf{1} = \begin{pmatrix} 1 & 0 & 0 & \cdots \\ 0 & 1 & 0 & \cdots \\ 0 & 0 & 1 & \cdots \\ \cdots & & & \\ \cdots & & & \end{pmatrix} \quad \text{and} \quad \boldsymbol{\Upsilon} = \begin{pmatrix} 1 & 1 & 1 & \cdots \\ 1 & 1 & 1 & \cdots \\ 1 & 1 & 1 & \cdots \\ \cdots & & & \\ \cdots & & & \end{pmatrix} \tag{4.7}$$

Note that the two matrices commute. Using these notations we get

$$\frac{2\boldsymbol{g}_T}{1 - \boldsymbol{g}_T + \boldsymbol{g}_R} = \frac{2\tau^2}{1 - \tau^2} \frac{1}{1 + \frac{\epsilon^2}{1-\tau^2}\boldsymbol{\Upsilon}} \tag{4.8}$$

$$= \frac{2\tau^2}{1 - \tau^2} \frac{1}{1 + \boldsymbol{c}\boldsymbol{c}^t} = \frac{2\tau^2}{1 - \tau^2}\left[\mathbf{1} - \frac{\epsilon^2 \tau^2}{(1-\tau^2)^2}\boldsymbol{\Upsilon}\right] \tag{4.9}$$

where we have defined the normalized column vector

$$c_a = \frac{\epsilon}{\sqrt{1 - \tau^2}} \qquad a = 1, 2, \cdots \mathcal{M} \tag{4.10}$$

and we have used the identity

$$\frac{1}{1 + \boldsymbol{c}\boldsymbol{c}^t} = \mathbf{1} - \frac{1}{1 + \boldsymbol{c}^t\boldsymbol{c}}\boldsymbol{c}\boldsymbol{c}^t = \mathbf{1} - \frac{1}{2}\boldsymbol{c}\boldsymbol{c}^t \tag{4.11}$$

Observing that $\sum_{ab} \mathbf{1}_{ab} = \mathcal{M}$ and $\sum_{ab} \boldsymbol{\Upsilon}_{ab} = \mathcal{M}^2$ we get the desired result Eq.(1.15).

Though the arguments above, are quite compelling, we were careful to verify that all the results that we find for the simplified network model are also applicable in the case of the

43

Sinai-type system of Fig. 6b where the scatterer is a semi-disc. This issue will be consider in chapter 5 We prefer in the present work to analyze the network model of Fig. 6d with Eq.(4.6) and not the semi-disc model of Fig.6b because the mathematics is much simpler, and the quality of the numerics is much better.

4.2   The quantum bound on G

We start the calculation of the conductance by writing the channel wavefunctions as $\Psi_a(x) = A_a \sin(kx + \varphi)$, where a labels the modes. In our simplified network model the modes are re-interpreted as bonds, and we assume that the wavevector $k = (2\mathsf{m}E)^{1/2}$ is the same for all bonds. For the matrix elements of $\mathcal{I}$ we have the expression

$$\mathcal{I}_{nm} \approx -iev_{\mathrm{F}} \sum_a \frac{1}{2} \mathsf{A}_a^{(n)} \mathsf{A}_a^{(m)} \sin(\varphi_a^{(n)} - \varphi_a^{(m)}) \tag{4.12}$$

were the approximation takes into account that our interest is in the couplings between levels with $k_n \approx k_m \approx k_{\mathrm{F}}$. From this expression we deduce that the scaled matrix elements of Eq.(2.20) are bounded as follows:

$$I_{nm} \quad < \quad \sum_a \frac{L}{2} \mathsf{A}_a^{(n)} \mathsf{A}_a^{(m)} \quad < \quad 1 \tag{4.13}$$

Therefore, irrespective of the details of the averaging or coarse graining procedure, it is clear that $g < 1$ as stated at the end of the previous section. Consequently

$$G\Big|_{\mathrm{maximal}} = \frac{e^2}{2\pi\hbar}\mathcal{M}^2 \tag{4.14}$$

In the last expression we have omitted a factor of 2. This is not a typo. We shall explain this point in section 4.10.

4.3 The ergodic result for G

The simplest hypothesis is that all the wavefunctions are ergodic random waves. This is in the spirit of Mott's derivation [37, 38], where it has been demonstrated that a random wave assumption recovers (via Eq.(2.18)) the Drude result. If indeed the wavefunctions were spread equally over all the bonds, it would imply $|\mathsf{A}_a|^2 \sim 2/(\mathcal{M}L)$. If this were true we would get

$$|I_{nm}|^2 \;\;=\;\; \left| \frac{1}{\mathcal{M}} \sum_a \sin(\varphi^{(n)} - \varphi^{(m)}) \right|^2 \;\;\approx\;\; \frac{1}{2\mathcal{M}} \tag{4.15}$$

This would imply

$$G\bigg|_{\text{ergodic}} \;\;=\;\; \frac{e^2}{2\pi\hbar}\mathcal{M} \tag{4.16}$$

We would like to argue that this result is wrong. Moreover, it must be wrong. The result is wrong because the eigenfunction of a ballistic ring are not ergodic. This we discuss in section 4.8. The result *must* be wrong because it violates quantum-classical correspondence, which we discuss in the next section.

4.4 The quantum conductance and Drude

In this section we define the distinction between mesoscopic and spectroscopic conductance and further discuss the latter. In section 4.5 we elaborate on the calculation procedure of both. We would like to clarify in advance that the spectroscopic conductance is the outcome of the traditional Kubo calculation. Moreover, it is only the spectroscopic conductance which obeys quantum-classical correspondence considerations.

Mesoscopic conductance: If the environmentally induced relaxation can be neglected, the rate of energy absorption depends on having *connected* sequences of transitions between levels [11]. In section 4.5 we explain the proper procedure for calculating the con-

ductance in such circumstances. The result that comes out from such calculation is what we call the mesoscopic conductance G_{meso}.

Spectroscopic conductance: Within the framework of linear response theory, it is assumed that the EMF-induced transitions are very slow compared with the environmentally induced relaxation. Then one can argue that Eq.(2.18) is valid with $\langle\langle|\mathcal{I}_{nm}|^2\rangle\rangle$ interpreted as an *algebraic average* over the matrix elements. This is what we called in section 2.3 the *traditional* Kubo formula. Optionally, if applicable, one may perform an algebraic average over realizations of disorder. The latter is a very common procedure in diagrammatic calculations. The outcome of the (traditional) calculation is what we call the spectroscopic conductance G_{spec}. For further discussion of the conditions that justify a "spectroscopic" calculation see Ref. [11].

The spectroscopic conductance is not very sensitive to Γ. In fact the Γ dependence of the result is nothing else but the weak localization correction [9]. It scales like Δ/Γ for diffusive rings, where Δ is the mean level spacing (note Eq.(2.19)).

Disregarding weak localization corrections it can be argued [11] that the obtained result for G_{spec} is G_{Drude} provided some reasonable quantum-to-classical correspondence conditions (see below) are satisfied. It follows that the ergodic hypothesis of the previous section cannot be correct, because G_{Drude} is definitely not bounded by the number of open modes - it can be much larger.

The necessary condition for quantum-classical correspondence can be deduced by taking into account the quantum bound of section 4.2. As g_T becomes closer to 1, the Drude expression diverges. Quantum-to-classical correspondence is feasible provided the quantum bound is not exceeded:

$$\frac{1}{1-g_T} \quad \ll \quad \mathcal{M} \tag{4.17}$$

This can be re-phrased as

$$\frac{\ell}{L} < \mathcal{M} \tag{4.18}$$

or as

$$t_{cl} \quad \ll \quad t_H \tag{4.19}$$

where $t_{cl} = \ell/v_{\mathrm{F}}$ is the ballistic time, and $t_H = \mathcal{M} \times (L/v_{\mathrm{F}})$ is the Heisenberg time (the time to resolve the quantized energy levels). In order to establish quantum-to-classical correspondence in a constructive manner one should express the Kubo formula using Green functions, leading to a double summation over paths. Then one should argue that energy averaging justify the use of the diagonal approximations. The procedure is the same as in [39].

4.5   The calculation of G

Within the framework of semi-linear response theory the recipe for calculating G is implied by the Fermi golden rule (FGR) picture. The Hamiltonian of the ring in the adiabatic basis is $\mathcal{H} \mapsto E_n \delta_{nm} + W_{nm}$ where $W_{nm} = i\dot{\Phi}\hbar\mathcal{I}_{nm}/(E_n - E_m)$, and $-\dot{\Phi}$ is the EMF. The FGR transition rate between level n and level m is

$$w_{nm} \quad = \quad \frac{2\pi}{\hbar}\delta(E_n - E_m)|W_{nm}|^2 \tag{4.20}$$

Since we are dealing with a closed system one should take explicitly into account the broadening of the delta function:

$$\delta(E_n - E_m) \quad \rightarrow \quad \frac{1}{\Gamma}F\left(\frac{E_n - E_m}{\Gamma}\right) \tag{4.21}$$

The normalized kernel $F()$ reflects either the power spectrum or the non-adiabaticity of the driving. For the purpose of numerical demonstration we assume $F(r) = \exp(-2|r|)$ as in [12]. The level broadening Γ is identical with Γ of Ref.[11, 33] and with $\hbar\omega_0$ of Ref.[12]. As in the conventional derivation of linear response theory, also here we regard Γ as a free parameter in the theory. It is convenient to use dimensionless quantities, so we re-write Eq.(4.21) as:

$$w_{nm} \quad = \quad \varrho_{\mathrm{F}}\frac{e^2}{\pi\hbar}\mathcal{M}^2\mathsf{g}_{nm}\dot{\Phi}^2 \tag{4.22}$$

47

where the dimensionless transition rates are

$$g_{nm} = \frac{|I_{nm}|^2}{(n-m)^2}\frac{1}{\gamma}F\left(\frac{n-m}{\gamma}\right) \tag{4.23}$$

and $\gamma = \Gamma/\Delta$ is the dimensionless broadening parameter. There is an implicit approximation in Eq.(4.23), namely $(E_n - E_m)/\Delta \approx (n-m)$, that underestimates exceptionally large couplings between almost degenerated levels. In practice it is not going to be reflected in the G_{meso} calculation (see below), because the latter is determined by the bottlenecks.

The FGR transitions between levels lead to diffusion in energy space. We would like to calculate the *coarse grained diffusion coefficient D* without assuming that all the w_{nm} are comparable. For this purpose it is useful to exploit the following resistor network analogy [12]

$$w_{nm}^{-1} \iff \text{resistor between node } n \text{ and node } m \tag{4.24}$$

$$D^{-1} \iff \text{resistivity of the network} \tag{4.25}$$

In dimensionless units w_{nm} is denoted as g_{nm} as defined via Eq.(4.22) In dimensionless units D is denoted as g and it is defined via the following equation:

$$D = \varrho_{\mathrm{F}}^{-1}\frac{e^2}{\pi\hbar}\mathcal{M}^2 g\dot{\Phi}^2 \tag{4.26}$$

The extra $\varrho_{\mathrm{F}}^{-2}$ factor compared with Eq.(4.22) arise because the resistivity D^{-1} is calculated per unit "energy length" while the scaled resistivity g^{-1} is per unit site.

A standard numerical procedure is used for extracting g for a given resistor network g_{nm}. The steps are as follows: **(i)** Cut an N site segment out of the network (Fig. 7). **(ii)** Define a vector $J_n (n = 1..N)$ whose elements are all zero except the first and the last that equal $J_1 = +J$ and $J_N = -J$. **(iii)** Solve the matrix equation

$$J_n = \sum_m g_{nm}(V_n - V_m) \tag{4.27}$$

This equation should be solved for V_n. In practice it is easier to write this equation as $J = -\tilde{g}V$ where $\tilde{g}_{nm} = g_{nm} - \delta_{nm}\sum_{m'} g_{nm'}$. The difference $V_1 - V_N$ is obviously proportional to

48

the injected J. **(iv)** Find the overall resistance of the truncated network $\mathbf{g}_N = J/(V_N - V_1)$. And finally: **(v)** Define the resistivity as $\mathbf{g}^{-1} = \mathbf{g}_N^{-1}/N$. For a locally homogeneous network it has been argued in Ref.[11] that $\mathbf{g}$ can be obtained via an harmonic average:

$$\mathbf{g}\Big|_{\text{meso}} \approx \left[\frac{1}{N} \sum_n^N \left[\frac{1}{2} \sum_m (m-n)^2 \mathbf{g}_{nm} \right]^{-1} \right]^{-1} \tag{4.28}$$

The internal sum reflects addition of resistors in parallel, while the harmonic average reflects addition of resistors in series. This should be contrasted with the algebraic average which is used in order to calculated the spectroscopic result:

$$\mathbf{g}\Big|_{\text{spec}} = \left[\frac{1}{N} \sum_n^N \left[\frac{1}{2} \sum_m (m-n)^2 \mathbf{g}_{nm} \right] \right] \tag{4.29}$$

From the diffusion-dissipation relation it follows that the rate of energy absorption equals $\varrho_{\text{F}} D$. Then it is implied by Eq.(1.1) that the conductance G is given by Eq.(2.21). The procedure above can be summarized by saying that $\mathbf{g}$ can be calculated form $|I_{nm}|^2$ via an appropriate "averaging procedure". The appropriate averaging procedure is *algebraic* Eq.(4.29) in the case of the spectroscopic conductance. The appropriate averaging procedure is *harmonic-type* (as discussed above) in the case of mesoscopic conductance. Schematically we write in both cases

$$\mathbf{g} = \langle\langle |I_{nm}|^2 \rangle\rangle \tag{4.30}$$

It should be clear that in both cases (spectroscopic, mesoscopic) the "averaging" requires the specification of the smoothing scale Γ as implied by Eq.(4.23). It is also clear that the mesoscopic result is much more sensitive to the value of Γ. Unlike the spectroscopic result where this sensitivity to Γ is merely a "weak localization correction", in the case of the mesoscopic result the dependence on Γ is a leading order effect.

4.6 The eigenstates of the network model

The network model that we have presented in section 4.1 is defined in terms of the scattering matrix $\boldsymbol{S}_{\text{D}}$, and the free propagation matrix $\boldsymbol{S}_{\text{W}}$,

$$
\boldsymbol{S}_{\text{D}} \;=\; \begin{pmatrix} \epsilon \exp\left(i\, 2\pi\, \frac{a\,b}{\mathcal{M}} \right) & \sqrt{1 - \mathcal{M}\epsilon^2}\,\delta_{a,b} \\ \sqrt{1 - \mathcal{M}\epsilon^2}\,\delta_{a,b} & -\epsilon \exp\left(-i\, 2\pi\, \frac{a\,b}{\mathcal{M}} \right) \end{pmatrix} \tag{4.31}
$$

$$
\boldsymbol{S}_{\text{W}} \;=\; \begin{pmatrix} 0 & e^{ikL_a}\,\delta_{ab} \\ e^{ikL_a}\,\delta_{ab} & 0 \end{pmatrix} \tag{4.32}
$$

The wavefunction can be written as

$$
|\psi\rangle \;\longmapsto\; \sum_{a=1}^{\mathcal{M}} \left(A_{La}e^{i\,k\,(x-L_a)} + A_{Ra}e^{-i\,k\,x} \right) \otimes |a\rangle. \tag{4.33}
$$

The set of amplitudes A_L and A_R that can be arranged as a column vector of length $2\mathcal{M}$. The linear equation for the eigenstates is

$$
\begin{pmatrix} A_L \\ A_R \end{pmatrix} = \boldsymbol{S}_{\text{W}}\,\boldsymbol{S}_{\text{D}} \begin{pmatrix} A_L \\ A_R \end{pmatrix} \tag{4.34}
$$

and the associated secular equation for the eigenvalues is

$$
\det\left[\, \boldsymbol{S}_{\text{W}}\,\boldsymbol{S}_{\text{D}} - 1 \,\right] \;=\; 0 \tag{4.35}
$$

In the absence of driving we have time reversal symmetry, and the unperturbed eigenfunctions can be chosen as real (see 4.7):

$$
|\psi\rangle \;\longmapsto\; \sum_{a=1}^{\mathcal{M}} A_a \sin(kx + \varphi_a) \otimes |a\rangle. \tag{4.36}
$$

The wavefunction is normalized as

$$
\sum_{a=1}^{\mathcal{M}} \int_0^{L_a} A_a^2 \sin^2(kx + \varphi_a)\, dx = 1 \tag{4.37}
$$

which implies

$$\sum_{a=1}^{\mathcal{M}} \frac{L_a}{2} A_a^2 \approx 1 \tag{4.38}$$

For a given g_T we can find numerically the eigenvalues and the eigenstates, thus obtaining a table

$$(k_n, \varphi_a^{(n)}, A_a^{(n)}) \qquad n = \text{level index} \tag{4.39}$$

For the numerical study we have chosen a network system consisting of $\mathcal{M} = 50$ bonds. The length of each bond is randomly selected in the range $L_a = 1 \pm 0.1$. We select the eigenvalues with $k_n \sim 2000$. The numerical results over the whole range of g_T values are presented in Figs. 8-11. In the following sections we discuss and analyze these results.

It is of course possible to determine analytically what are the eigenvalues and the eigenstates in the $g_T \to 1$ limit. The combined scattering matrix is

$$\boldsymbol{S}_{\mathrm{W}}\, \boldsymbol{S}_{\mathrm{D}} = \begin{pmatrix} \tau\, \mathrm{e}^{ikL_a}\delta_{a,b} & -\epsilon\, \mathrm{e}^{i(kL_a - \frac{2\pi}{\mathcal{M}}a\times b)} \\ \epsilon\, \mathrm{e}^{i(kL_a + \frac{2\pi}{\mathcal{M}}a\times b)} & \tau\, \mathrm{e}^{ikL_a}\delta_{a,b} \end{pmatrix} \tag{4.40}$$

where we use the notation $\tau = (1 - \mathcal{M}\epsilon^2)^{1/2}$. For $g_T = 1$ this matrix becomes diagonal. Then it has $\mathcal{M}$ distinct eigenvalues, each doubly degenerate. We are interested in the non-degenerate case in the limit $\epsilon \to 0$. The eigenstates are still localized each in a single a bond, but the degeneracy is lifted. Within the framework of degenerate perturbation theory we have to diagonalize the 2×2 matrix

$$\begin{pmatrix} \tau\, \mathrm{e}^{ikL_a} & -\epsilon\, \mathrm{e}^{i(kL_a - \frac{2\pi\, a^2}{\mathcal{M}})} \\ \epsilon\, \mathrm{e}^{i(kL_a + \frac{2\pi\, a^2}{\mathcal{M}})} & \tau\, \mathrm{e}^{ikL_a} \end{pmatrix} \tag{4.41}$$

whose eigenvalue are determined by the associated secular equation

$$(\epsilon^2 + \tau^2)\mathrm{e}^{2ikL_a} - 2\tau\mathrm{e}^{ikL_a} + 1 = 0 \tag{4.42}$$

Hence we get the following approximations

$$k_n \approx \left(2\pi \times \text{integer} \pm \frac{1}{\sqrt{\mathcal{M}}} \, \epsilon \right) \frac{1}{L_a} \tag{4.43}$$

$$\varphi_a^{(n)} \approx -\frac{a^2}{\mathcal{M}} \pi - \frac{1}{2} k_n L_a + \begin{cases} \pi/4 \\ 3\pi/4 \end{cases} \tag{4.44}$$

We have verified that the numerical results of Fig. 8 and Fig. 11 agree with these estimates. We note that for hard wall scatterer each φ_a would become either 0 or $\pi/2$ in the $g_T \to 1$ limit.

4.7 Implications of time reversal symmetry

We can decompose the eigenstate equation as follows:

$$\begin{pmatrix} B_{La} \\ B_{Ra} \end{pmatrix} = S_{\mathrm{D}} \begin{pmatrix} A_{La} \\ A_{Ra} \end{pmatrix} \tag{4.45}$$

$$\begin{pmatrix} A_{La} \\ A_{Ra} \end{pmatrix} = S_{\mathrm{W}} \begin{pmatrix} B_{La} \\ B_{Ra} \end{pmatrix} \tag{4.46}$$

Above B_{La} and B_{Ra} are the amplitudes of the outgoing waves from $x = 0$, while A_{La} and A_{Ra} are the amplitudes of the ingoing waves. Conventional time-reversal-symmetry implies that both $\psi(x)$ and its complex-conjugate $\psi(x)^*$ satisfy the same Schrödinger equation. Complex conjugation turns out the incoming wave into outgoing one and vice verse, and therefore

$$\begin{pmatrix} A_{La}^* \\ A_{Ra}^* \end{pmatrix} = S_{\mathrm{D}} \begin{pmatrix} B_{La}^* \\ B_{Ra}^* \end{pmatrix} \tag{4.47}$$

$$\begin{pmatrix} B_{La}^* \\ B_{Ra}^* \end{pmatrix} = S_{\mathrm{W}} \begin{pmatrix} A_{La}^* \\ A_{Ra}^* \end{pmatrix} \tag{4.48}$$

It is not difficult to see that the two sets of equations are equivalent provided

$$S_{\mathrm{D}}^{\text{transposed}} = S_{\mathrm{D}} \tag{4.49}$$

$$S_{\mathrm{W}}^{\text{transposed}} = S_{\mathrm{W}} \tag{4.50}$$

If we have this (conventional) time reversal symmetry, the unperturbed eigenfunctions can be chosen as real in position representation:

$$|\psi\rangle = \sum_{a=1}^{\mathcal{M}} A_a \sin(kx + \varphi_a) \otimes |a\rangle. \tag{4.51}$$

where

$$A_a = 2|A_{La}| = 2|A_{Ra}| \tag{4.52}$$

$$\varphi_a = \frac{1}{2}\left(\pi + \arg(A_{La}/A_{Ra}) - kL_a\right) \tag{4.53}$$

4.8 The non-ergodicity of the eigenfunctions

In Fig. 9 we display images of the column vectors $A_a^{(n)}$ for two representative values of g_T so as to illustrate the crossover from localized to ergodic wavefunctions. Each eigen-function can be characterized by its participation ratio:

$$\text{PR} = \left[\sum_a \left(\frac{L_a}{2}A_a^2\right)^2\right]^{-1} \tag{4.54}$$

This constitutes a measure for the ergodicity of the eigen-functions. By this definition

$$\text{PR} \approx \begin{cases} 1 & \text{for a single bond localized state} \\ \mathcal{M} & \text{for a uniformly distributed state} \end{cases} \tag{4.55}$$

We distinguish between 3 regimes depending on the value of the total transmission g_T,

- The trivial ballistic regime $(1 - g_T) \ll 1/\mathcal{M}$ for which PR ~ 1

- The non-trivial ballistic regime $1/\mathcal{M} \ll (1 - g_T) \ll 1$.

- The non-ballistic regime where g_T is not close to 1 and PR $\sim \mathcal{M}$

53

In the trivial ballistic regime the eigenstates are like those of a reflection-less ring with uncoupled modes, hence PR ~ 1. Once $(1 - g_T)$ becomes larger compared with $1/\mathcal{M}$ first order perturbation theory breaks down, and the mixing of the levels is described by a Wigner Lorentzian. The analysis is completely analogous to that of the single mode case of Ref.[11], leading to PR $\propto (1 - g_T) \times \mathcal{M}$. For g_T values that are not close to 1 the eigen-functions become ergodic with PR $\sim \mathcal{M}$. From RMT we expect [40] PR $\sim \mathcal{M}/3$. A satisfactory global fit, that works well within the non-trivial ballistic regime is (Fig. 12):

$$\text{PR} \approx 1 + \frac{1}{3}(1 - g_T)\mathcal{M} \tag{4.56}$$

Our interest is focused in the *non-trivial* ballistic regime $1/\mathcal{M} \ll (1 - g_T) \ll 1$, where we have strong mixing of levels (PR $\gg 1$), but still the mean free path $\ell \approx L/(1 - g_T)$ is very large compared with the ring's perimeter ($\ell \gg L$). It is important to realize that in this regime we do not have "quantum chaos" ergodicity. Rather we have PR $\ll \mathcal{M}$ meaning that the wavefunctions occupy only a small fraction of the classically accessible phase space.

4.9 The calculation of matrix elements

Given a set of eigenstates, it is straightforward to calculate the matrix elements of the current operator (Figs. 13-16). We recall that the scaled matrix elements are

$$I_{nm} \approx \sum_a \frac{L_a}{2} A_a^{(n)} A_a^{(m)} \sin(\varphi_a^{(n)} - \varphi_a^{(m)}) \tag{4.57}$$

with the associated upper bound

$$\bar{I}_{nm} \approx \sum_a \frac{L_a}{2} A_a^{(n)} A_a^{(m)} \tag{4.58}$$

For $n = m$ we have $\bar{I}_{nm} = 1$ due to normalization, and $I_{nm} = 0$ due to time reversal symmetry. From now on we are interested in $n \neq m$. There are several extreme cases that

allow simple estimates:

$$\bar{I}_{nm} \approx \begin{cases} 0 & \text{for pair of states localized on different bonds} \\ 1 & \text{for pair of states localized on the same bond} \\ 1 & \text{for pair of ergodic states} \end{cases}$$

If we take the phases into account we get

$$|I_{nm}|^2 \approx \begin{cases} 0 & \text{for pair of states localized on different bonds} \\ 1 & \text{for pair of nearly degenerated states on the same bond} \\ 1/(2\mathcal{M}) & \text{for pair of uncorrelated ergodic states} \end{cases}$$

We have already explained in section 4.3 that the "ergodic" hypothesis is wrong in the ballistic case. It should be clear that the small PR of the eigenfunctions implies sparsity of I_{nm}: The matrix elements are very small for any pair of states that are localized on different sets of bonds. This observation is demonstrated in Figs. 13-16. As the reflection $1 - g_T$ is increased, more and more elements become non-negligible, and the matrix becomes less structured and less sparse.

4.10   Numerical results for the conductance

Once we have the matrix elements $|I_{nm}|^2$ we can calculate G_{spec} using the algebraic average recipe Eq.(4.29). We can also calculate G_{meso} using either the resistor network procedure or the harmonic average approximation Eq.(4.28). Fig. 17 displays the results for an $\mathcal{M} = 50$ network model. The dependence on Γ is plotted in Fig. 18, and the rough accuracy of the harmonic average approximation is demonstrated in Fig. 19.

The dependence of G on the smoothing parameter Γ is easily understood if we keep in our mind the band profile which is illustrated in Fig. 14. In order to improve our intuition we show in Fig. 16 the average value of $|I_{n,n+r}|^2$ for $r = 1, 2, 3, 4, 5$ as a function of $1 - g_T$ for $r = 1, 2, 3, 4, 5$.

It should be clear that the large $r = 1$ elements originate from the pairs of almost degenerate states that were discussed in section 4.6. Their contribution to the spectroscopic conductance is dominant. The upper bound Eq.(4.14) on G is implied by the upper bound on $|I_{n,n+1}|^2$. It was already pointed out in section 4.9 that the maximal value $|I_{nm}| = 1$ is attained for the nearly degenerate states. The algebraic average with the interlacing vanishingly small couplings leads to the factor of $1/2$ that was mentioned after Eq.(4.14).

On the other hand, the large $r = 1$ couplings almost do not affect the mesoscopic conductance. This is because they do not form connected sequences. Moreover, as implied by our calculation recipe, large value of Γ cannot help to overcome the bottlenecks. In order to get a classical result the environment should induce not only level broadening (which is like the $1/T_2$ rate of pure dephasing in NMR studies), but also a relaxation effect (analogous to the $1/T_1$ rate in NMR).
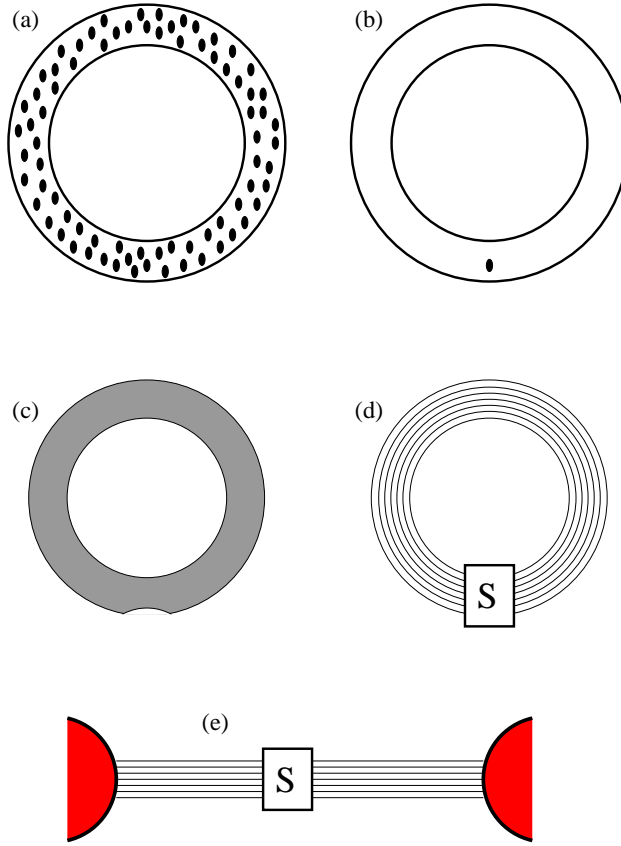
Fig.5: (a) A ring with disorder. The mean free path can be either $\ell \ll L$ for diffusive ring or $\ell \gg L$ for ballistic ring, where L is the length of the ring. **(b)** A chaotic ballistic ring. Here we have a single scatterer. The annular region supports $\mathcal{M}$ open modes. **(c)** Another version of a chaotic ring. Here the scattering is due to a deformation of the boundary. **(d)** A chaotic ring can be regarded as a network. Namely, each bond corresponds to an open mode. In the numerics the lengths of the bonds $(0.9 < L_a < 1.1)$ are chosen in random. The scattering is described by an S matrix. **(e)** The associated open (leads) geometry which is used in order to define the S matrix and the Landauer conductance.
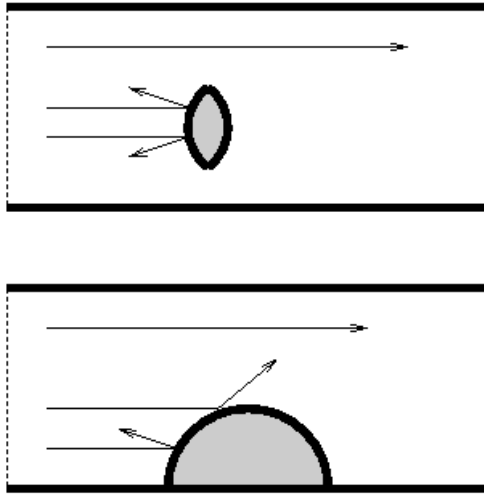
Fig.6: (a) upper panel: a waveguide with convex scatterer. This geometry has inspired our simple network model. **(b)** lower panel: the semi disc model. For this geometry we have some preliminary numerical results.
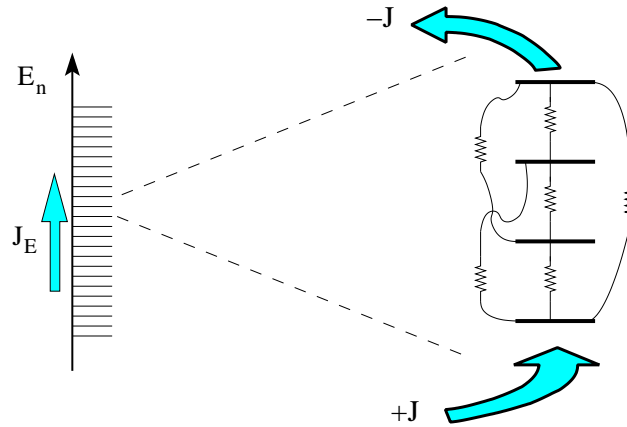
Fig.7: Within the framework of the Fermi golden rule picture the flow of the probability current in a multi level system is analogous to the flow of current via a resistor network. Thus the inverse of the course grained diffusion coefficient can be re-interpreted as the resistivity of the network. On the right we display a truncated segment, where $+J$ is the current injected from one end of the network, while $-J$ is the same current extracted from the other end. The injected current to all other nodes is zero. The resistance of each "resistors" in the network corresponds to g_{nm}^{-1}.
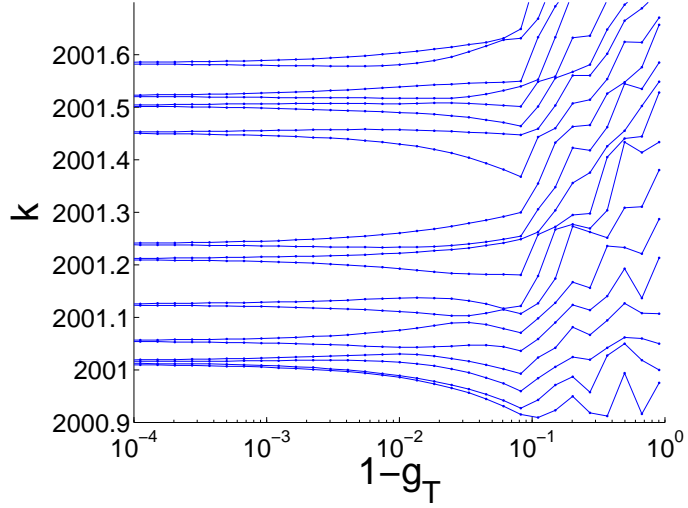
Fig.8: The eigenvalues k_n within a small energy window around $k \sim 2000$ are shown as a function of the reflection $1 - g_T$. We consider here a network model with $\mathcal{M} = 50$ bonds. The length of each bond was chosen in random within $0.9 < L_a < 1.1$.
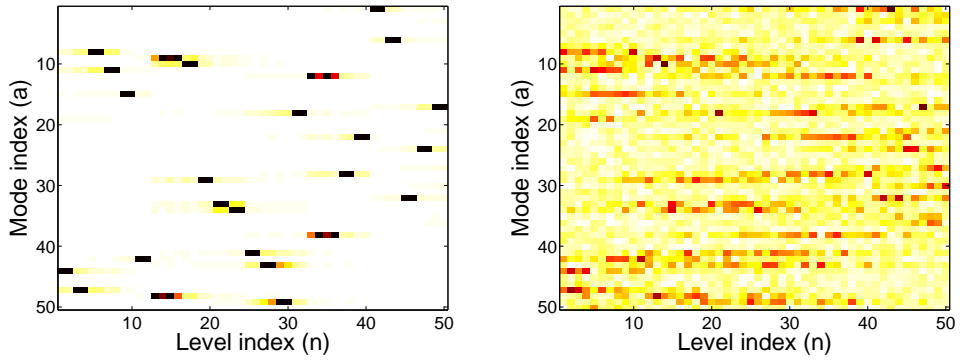

Fig.9: Each column is a gray level image of one eigenvector $|A_a^{(n)}|^2$, where $a = 1..\mathcal{M}$ is the bond index. We display the eigenvectors in the range $2000 < k < 2031$. Left panel: $g_T = 0.999$. Right panel: $g_T = 0.5$.
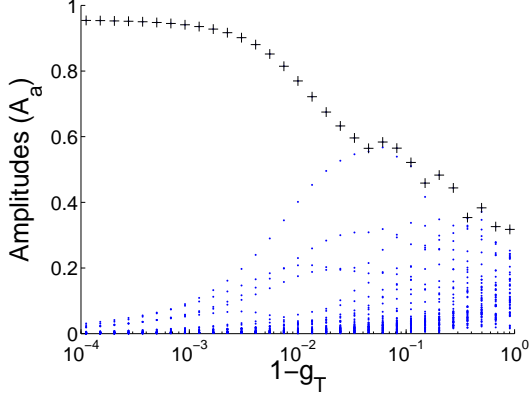
59

Fig.10: The amplitudes $|A_a^{(n)}|^2$ with $a = 1...\mathcal{M}$ of one representative state ($k_n \approx 2011$) as a function of the reflection. The wavefunction is localized on a single bond for small reflection, and becomes ergodic for large reflection.
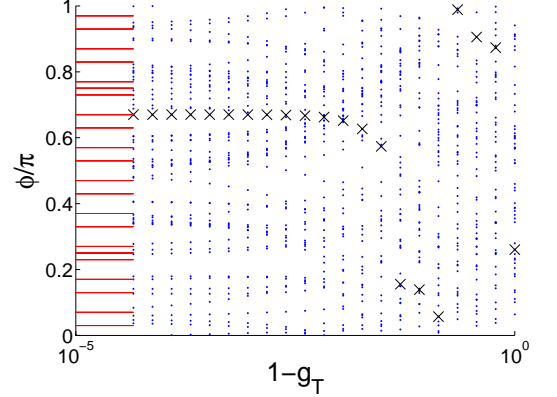

Fig.11: The phases $\varphi_a^{(n)}$ for the same eigenstate of Fig. 8. The solid lines are the values which are implied by Eq.(4.44). The crosses indicate the phases within the bond a where most of the wavefunction is localized. Indeed in the limit $g_T \to 1$ this phase coincides with one of the predicted values.
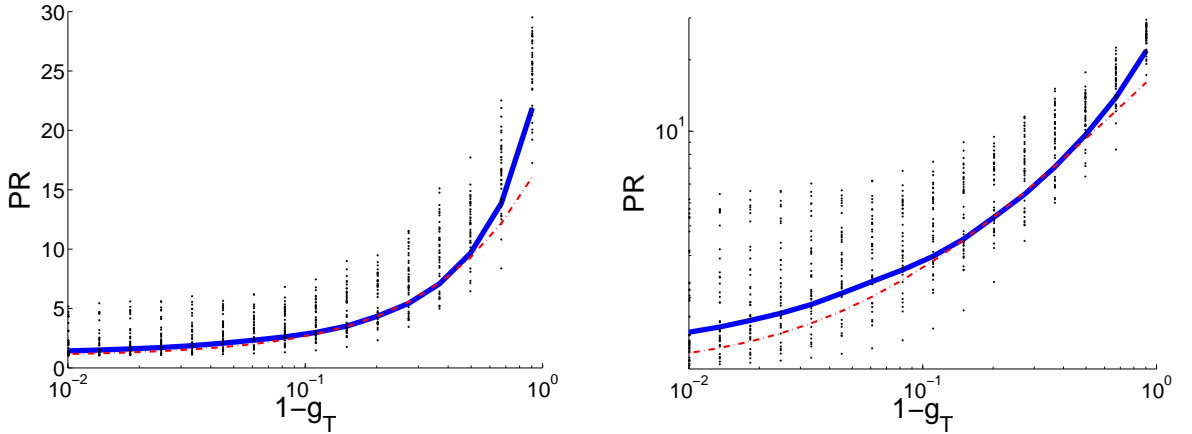

Fig.12: For each value of g_T we calculate the participation ratio (PR) for all the eigenstates. We display a set of randomly chosen representative value. The solid line is the average PR, and the dotted line is Eq.(4.56).
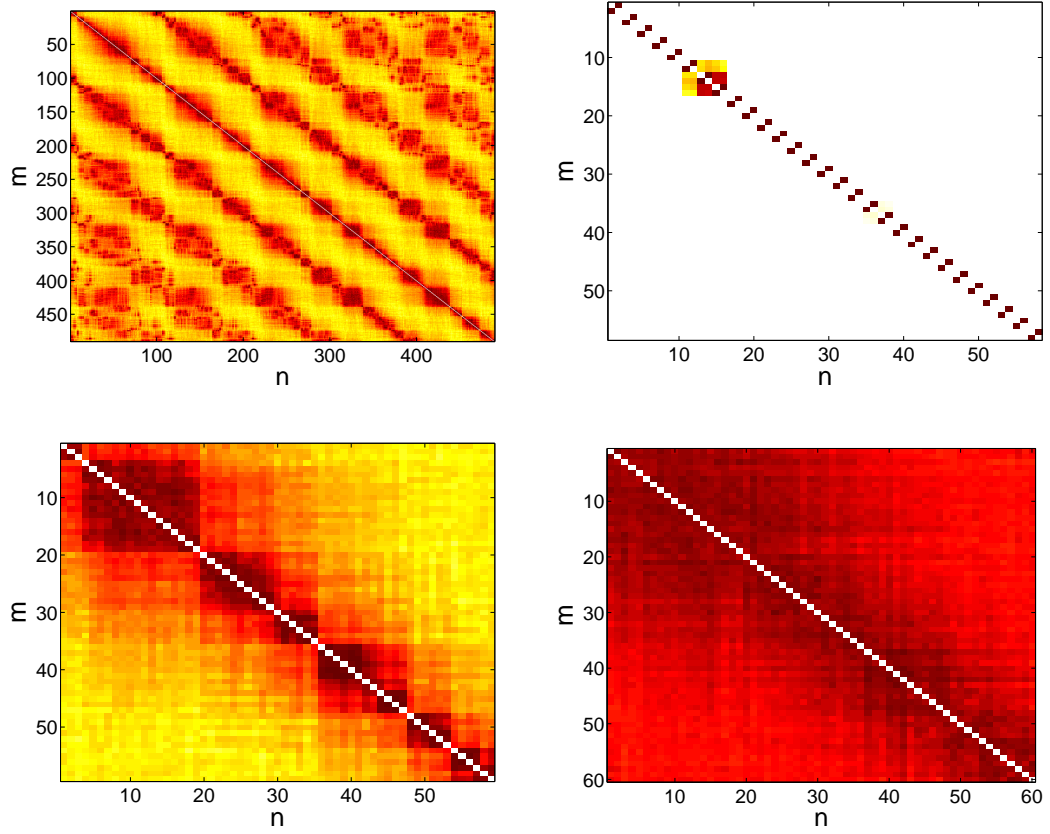
Fig.13: Images of $|\bar{I}_{nm}|^2$. The main diagonal is eliminated from the image. In left upper panel we display a relatively large representative piece for $g_T = 0.9$. In the other panels we display zoomed images for $g_T = 0.999, 0.9, 0.5$. As the reflection $1 - g_T$ becomes larger, more elements become non-negligible, and the matrix becomes less structured and less sparse.
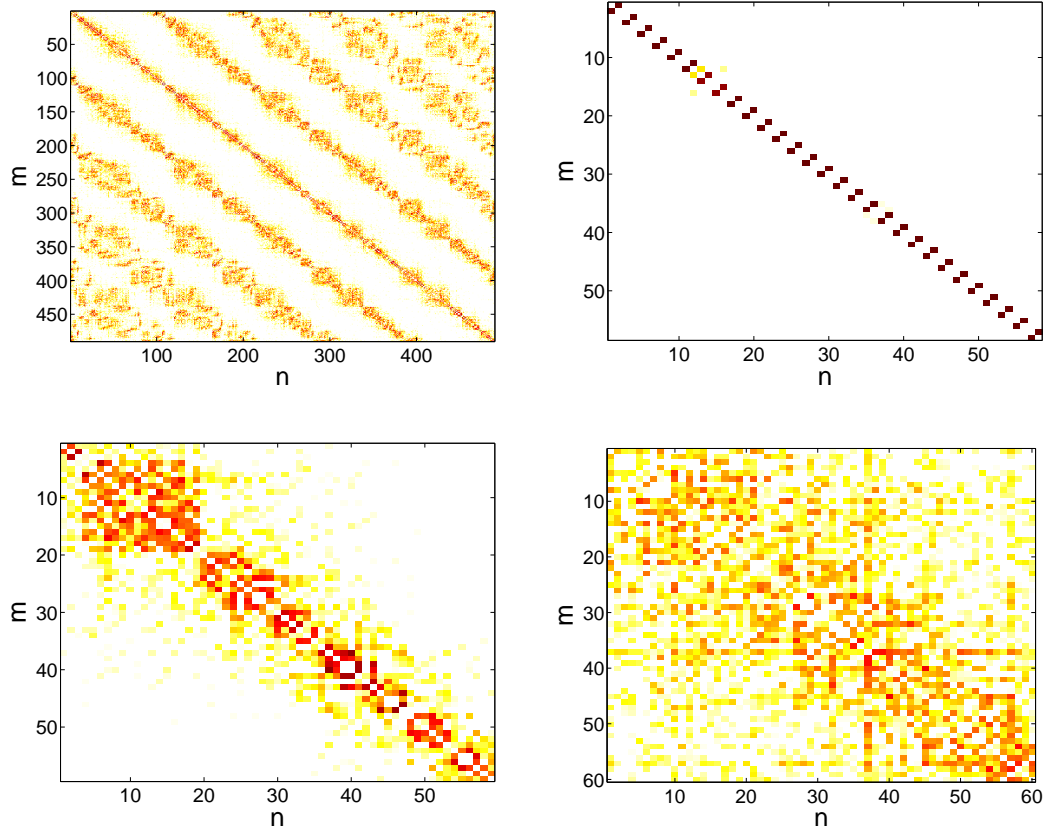
Fig.14: Images of $|I_{nm}|^2$. The main diagonal is zero due to time reversal symmetry. In left upper panel we display a relatively large representative piece for $g_T = 0.9$. In the other panels we display zoomed images for $g_T = 0.999, 0.9, 0.5$. As the reflection $1 - g_T$ becomes larger, more elements become non-negligible, and the matrix becomes less structured and less sparse.
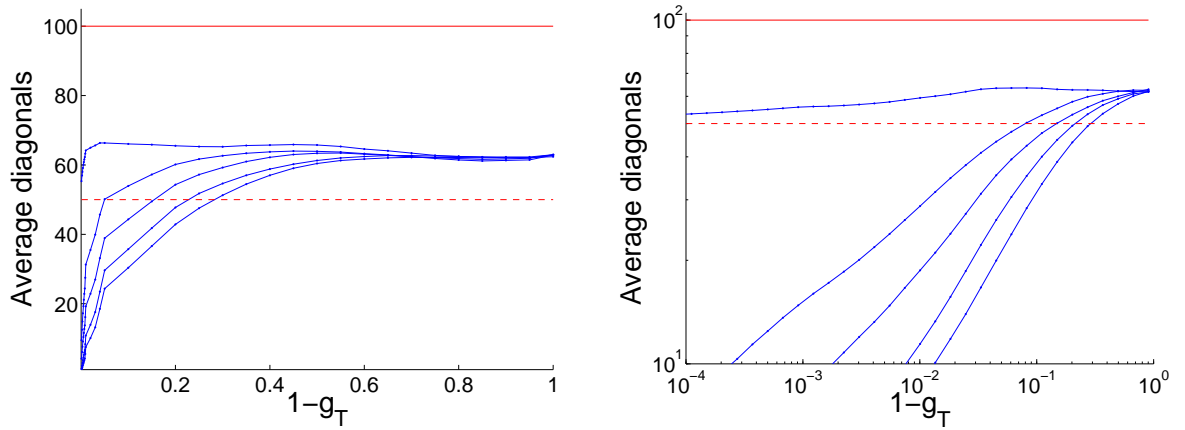
Fig.15: The n-averaged value of $2\mathcal{M}|\bar{I}_{n,n+r}|^2$ as a function of $1 - g_T$ for $r = 1, 2, 3, 4, 5$. The ergodic value for this quantity ($2\mathcal{M}$) is indicated by the solid horizontal line. We also indicate the value $\mathcal{M}$ by a dashed horizontal line. The left panel is normal scale, while the right panel is log-log.
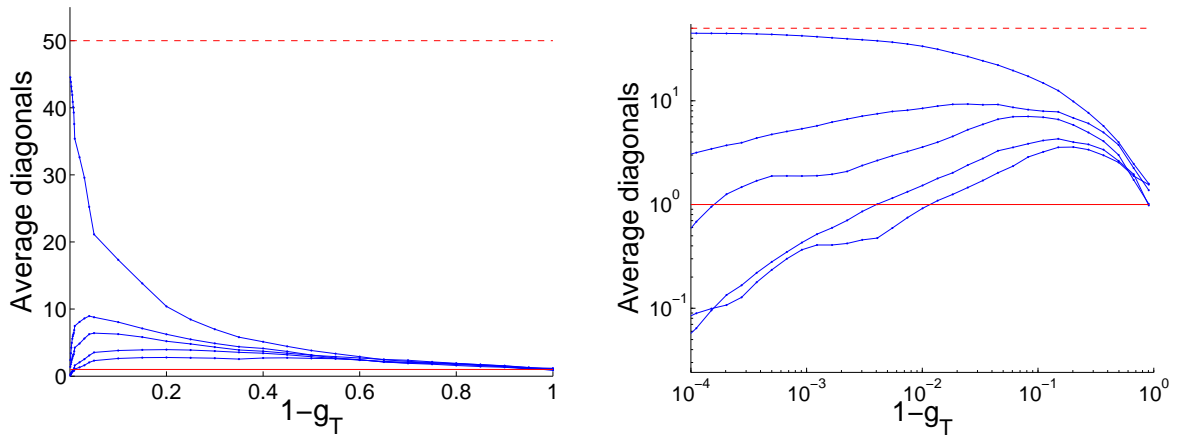

Fig.16: The n-averaged value of $2\mathcal{M}|I_{n,n+r}|^2$ as a function of $1 - g_T$ for $r = 1, 2, 3, 4, 5$. The ergodic value for this quantity (1) is indicated by the solid horizontal line. We also indicate the maximal value $\mathcal{M}$ by a dashed horizontal line. The left panel is normal scale, while the right panel is log-log.
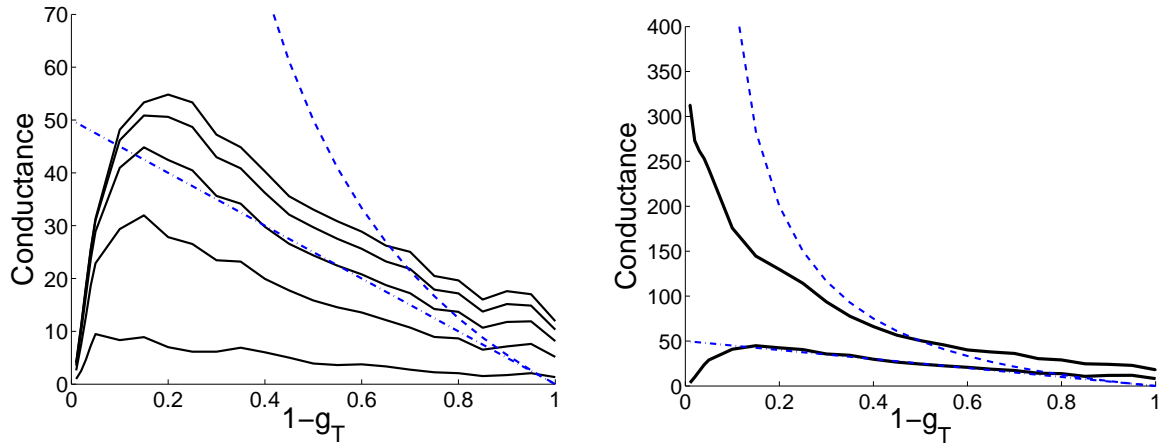
Fig.17: (a) Left panel: The mesoscopic conductance G in units of $e^2/(2\pi\hbar)$ as a function of $1 - g_T$. The curves from bottom to top are for $\gamma = 1, 2, 3, 4, 5$. The total number of open modes is $\mathcal{M} = 50$. The dotted line is G_{Landauer} while the dashed line is G_{Drude}. **(b)** Right panel: The mesoscopic conductance (lower solid line) is compared with the spectroscopic conductance (upper solid line). Here $\gamma = 3$. The dotted and the dashed lines are as in the left panel.
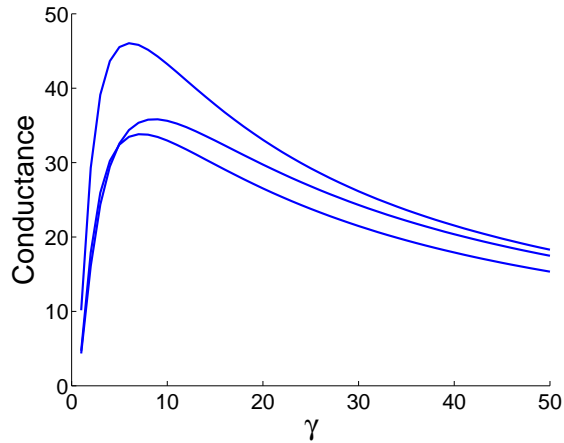

Fig.18: The mesoscopic conductance as a function of γ. The curves from top to bottom are for $g_T = 0.8, 0.7, 0.5$. The number of open channels is $\mathcal{M} = 50$.
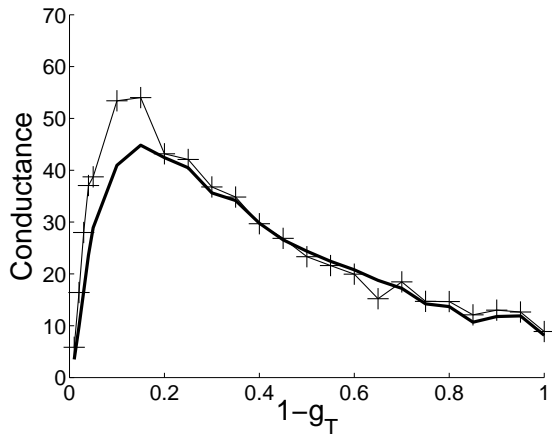
Fig.19: Left panel. The results for the mesoscopic conductance (solid line), as obtained via the resistor network procedure, are compared with the harmonic average approximation (crosses). The energy broadening parameter is $\gamma = 3$.

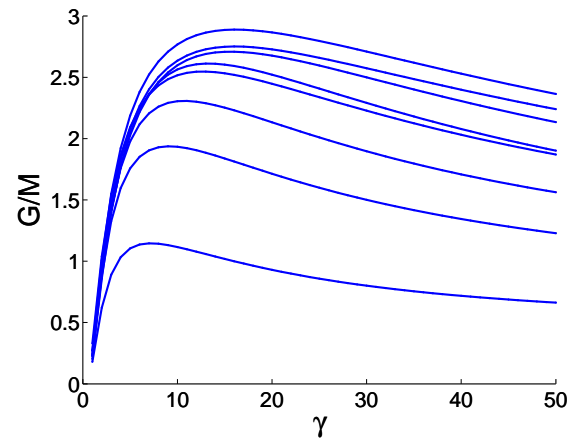**Fig.20:** The mesoscopic conductance divided by the number of channels as a function of gamma. The curves are from bottom to top $\mathcal{M} = 50, 100, 150, 200, 250, 300, 350, 400, 450$. The transition is $g_T = 0.8$, and the length of the network segment is $N = 400$. We were not able to determine wethere the conductance over the number of open modes saturate to a limit or is it weakly diverge

Chapter 5

Ballistic conductance of a ring with a semidisc scatterer

One can wonder whether the S matrix we have used in the previous chapter is 'generic', or maybe that model is over simplistic. In order to illuminate this point we consider the Sinai billiard models of Fig.6(a). These models are fully qualified as "quantum chaos" system as explained in previous chapter.

5.1   The model

Instead of a network consist of $\mathcal{M}$ wires connected at a single point by an $\boldsymbol{S}$ matrix as in the previous section, we consider waveguide of width W and length L closed to a ring, and $W \ll L$.

The width of the waveguide can support $\mathcal{M}$ open modes, each with different wavenumber in the transverse direction $k_a^t = \frac{pi}{W}a$, where a is the mode index. The wavenumber alone the ring will be

$$k_a = \sqrt{2\mathsf{m}E - \left(\frac{\pi}{W}a\right)^2} \quad a = 1, 2, ... \mathcal{M} \tag{5.1}$$

Alone the waveguide we have a semidisc scatterer of radius ϵ. We work with units such that $W = \mathsf{m} = \hbar = 1$, so the free parameters are $\mathcal{M}$, ϵ and L. We use the notation $k_E = \sqrt{2\mathsf{m}E}$. Given a desired number $\mathcal{M}$ and desired number of energy levels N, we can define an energy window.

$$E_{min} = \frac{1}{2\mathsf{m}} \left(\frac{\pi}{W}\mathcal{M}\right)^2 \tag{5.2}$$

$$E_{max} = E_{min} + N\frac{1}{\mathsf{g}(E)} \tag{5.3}$$

Where $\mathsf{g}(E)$ is the density of states. To find it we notice that the total number of energy level up to levels n, a is

$$E = \frac{1}{2\mathsf{m}} \left((\frac{\pi a}{W})^2 + (\frac{2\pi n}{L})^2\right) \tag{5.4}$$

For a constant energy this an ellipse equation with area

$$\Sigma(E) = \frac{\mathsf{m}EWL}{2\pi} \tag{5.5}$$

The density of state is $\mathsf{g}(E) = \partial_E \Sigma(E)$ divided by 4 to consider positive indices, and multiply by 2 to consider the degeneracy of the ring.

$$\mathsf{g} = \frac{\mathsf{m}WL}{2\pi} \tag{5.6}$$

$$\tag{5.7}$$

5.2 Classical transition matrix

In this section we calculate the classical transition matrix. The classical propagation angle as in the following plot is

$$\tan(\theta_a) = \frac{a}{\sqrt{2\mathsf{m}E(W/\pi)^2 - a^2}} \tag{5.8}$$
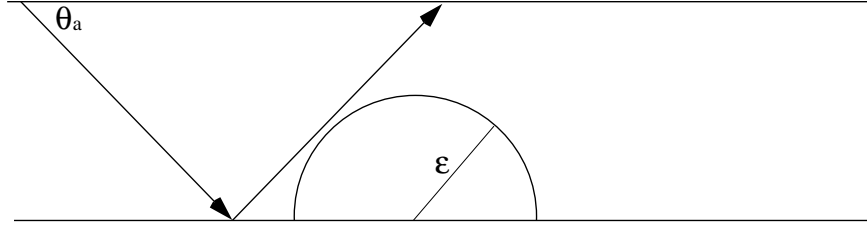
Fig.21 Classical trajectory of a particle in the waveguide

We calculated the trajectories of an incoming particle in channel a. The step size of that particle is $2W \cot(\theta_a)$, the effective length for scattering from the semidisc is $\frac{2\epsilon}{\sin(\theta_a)}$. So the probability of that particle to be scattered is $\frac{\epsilon}{W \cos(\theta_a)}$.

We consider the section of the step from which the particle is scattered, separate this section to small segments, for each segment we calculate the particle trajectory after it hit the scatterer. We check weather it is reflected or transmitted from the semidisk, or, if the the particle is still in the scattering area we consider the trajectory of a second scattering, and so on until the particle is transmitted or reflected from the semidisc. We repeat this numeric procedure for each segment in the section and for each mode a. Combining the results we can find the total probability of an incoming particle to be either reflected, transmitted or not to be scattered, as a function of the disk radius ϵ.

An approximate calculation can be done by neglecting the possibility for multipole scattering. Then we can calculate the transition matrix $\boldsymbol{g}$ directly. For that we can find, for each incoming particle with mode a the points on the section from which it is reflected to mode b. That points are at

$$q_a(b)^{\pm} = \frac{\epsilon}{\sin(\theta_a)} \sin\left(\frac{\pm\theta_b - \theta_a}{2}\right) \tag{5.9}$$

Then $\boldsymbol{g}_{ab}^{R}$, the probability to be reflected from mode a to mode b, is the sum of the derivatives of those point with respect to b divided by the total length of the step. In similar way we can find $\boldsymbol{g}_{ab}^{T}$, and add to it the unscattering probability, with the results.

$$\boldsymbol{g}_{ab}^R = \epsilon/(2Wm)\cos(\theta_a)\tan(\theta_b)\cos(\theta_a/2)\cos(\theta_b/2) \tag{5.10}$$

$$\boldsymbol{g}_{ab}^T = \begin{cases} \epsilon/(2Wm)\cos(\theta_a)\tan(\theta_b)\sin(\theta_a/2)\cos(\theta_b/2) & \text{For} \quad a > b \\ \epsilon/(2Wm)\cos(\theta_a)\tan(\theta_b)\cos(\theta_a/2)\sin(\theta_b/2) + \delta_{ab}(1 - \epsilon/(W\cos(\theta_a))) & \text{For} \quad a \leq b \end{cases} \tag{5.11}$$

In the following we plot a representative transition matrix.

$$\boldsymbol{g} = \begin{pmatrix} \boldsymbol{g}^R & \boldsymbol{g}^T \\ \boldsymbol{g}^T & \boldsymbol{g}^R \end{pmatrix} \tag{5.12}$$
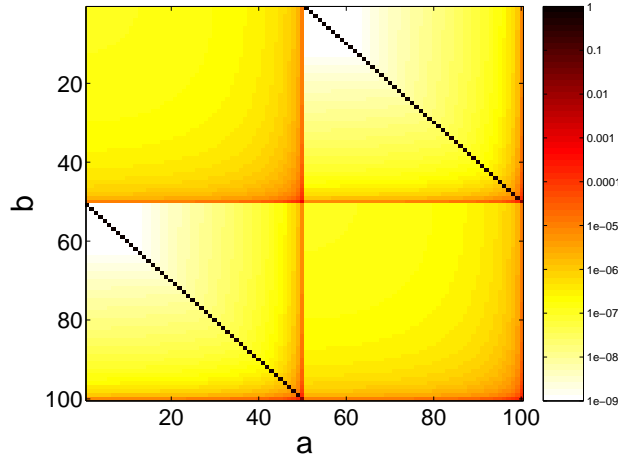

Fig.22 The transition matrix $\boldsymbol{g}$ for $\epsilon = 0.1$

In the following we plot the calculated probabilities, we can see that for small sized ϵ, which is the region we are interested, the approximation is satisfactory.

69
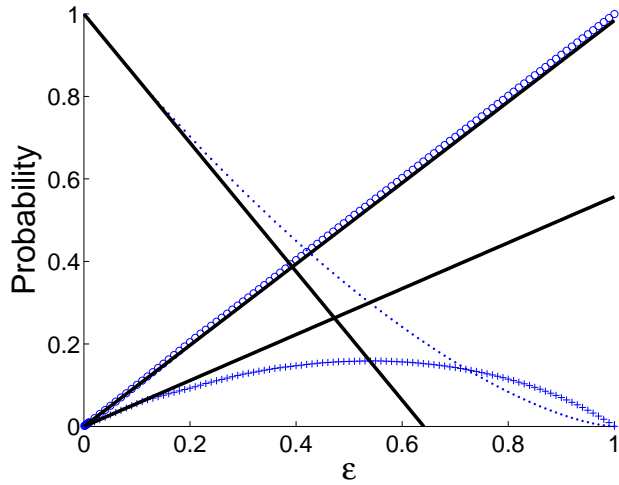
Fig.23 The probability to be reflected (circles), transmitted (crosses) and unscattered (dots) as a function of the semidisc radius ϵ. The thick lines are the corresponding probabilities using the approximation.

5.3   Quantal S matrix

In previous section we have calculate the scattering with semiclassical consideration, now we repeat the calculation for fully quantize system.

We are consider the waveguide with Dirichlet boundary condition on both sides, and a semidisc with Dirichlet boundary condition and radius ϵ center at $x = y = 0$, as in the following figure.

Fig.24 The semidisc system

The wavefunction in the system's different regions, when we assume in general an incoming mode a from the left direction and use polar coordinate decomposition for the region near the semidisc.

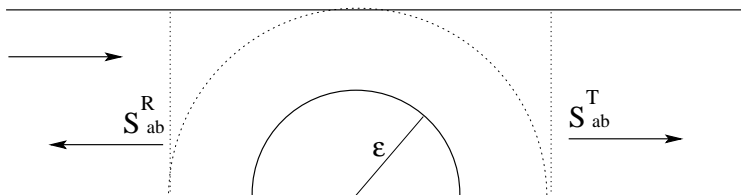$$\Psi_a(x < -\epsilon, y) \;=\; \frac{1}{\sqrt{k_a}}\chi_a(y)e^{ik_a x} + \sum_{b=1}^{\infty} \boldsymbol{S}_{ab}^R \frac{1}{\sqrt{k_b}}\chi_b(y)e^{-ik_b x} \tag{5.13}$$

$$\Psi_a(x > +\epsilon, y) \;=\; \sum_{b=1}^{\infty} \boldsymbol{S}_{ab}^T \frac{1}{\sqrt{k_b}}\chi_b(y)e^{ik_b x} \tag{5.14}$$

$$\Psi_a(r < W, \phi) \;=\; \sum_{l=-\infty}^{+\infty} a_{al} R_l(r)e^{il\phi} \tag{5.15}$$

Where we define $\chi(y)$ as the transverse wave function

$$\chi_a(y) = \sqrt{\frac{2}{W}}\sin(\frac{a\pi}{W}y) \tag{5.16}$$

$k_a = \sqrt{2mE - (\pi a/W)^2}$ is the wavenumber and $\boldsymbol{S}_{ab}^T$, $\boldsymbol{S}_{ab}^R$ are the elements of the scattering $\boldsymbol{S}$ matrix. In the coordinate decomposition we write the wavefunction as a sum of incoming and outgoing waves

$$R_l(r) = J_l(k_E r) + T_l H_l^+(k_E r) \tag{5.17}$$

Where T, the elastic reaction matrix, which is diagonal in the angular representation.

$$T_{ll'} = i(S_{ll'} - \delta_{ll'}) = ie^{i\sigma_l}\sin(\sigma_l)\delta_{ll'} \tag{5.18}$$

And σ_l is the scattering phase shift which for hard wall is

$$\tan(\sigma_l) = -\frac{J_l(k_E\epsilon)}{N_l(k_E\epsilon)} \tag{5.19}$$

We will find the coefficients a_{al} as in [36] by substituting into Lippman-Schwinger equation the radial wavefunction equation and the green function equation found at Ref. A of [35]

$$G(\mathbf{r}, \mathbf{r}') = \pi \sum_{ll'=-\infty}^{\infty} (\delta_{ll'} H_{l'}(k_E r) + F_{l-l'}(2Wk_E) J_l(kr)) J_{l'}(k_E r') e^{i(l\phi - l'\phi')} \tag{5.20}$$

$$F_l(2Wk_E) = 2 \sum_{n=1}^{\infty} \cos(l\frac{\pi}{2}) H_l(2nWk_E) \tag{5.21}$$

The Lippman-Schwinger equation

$$\Psi_a(\mathbf{r}) = \frac{1}{\sqrt{k_a}} e^{i\mathbf{k}\mathbf{r}} - \frac{\mathsf{m}}{2\pi} \int d^2\mathbf{r} \, G(\mathbf{r}, \mathbf{r}') V(\mathbf{r}') \Psi_a(\mathbf{r}') \tag{5.22}$$

We expand the free waves term, where $cos(\theta_a) = k_a/k_E$ is the wavenumber angle

$$e^{i\mathbf{k}\mathbf{r}} = \sum_l i^l J_l(k_E r) e^{il(\phi - \theta_a)} \tag{5.23}$$

And get the linear equation for the coefficient

$$\sum_{l'=-\infty}^{+\infty} (\delta_{ll'} - F_{l-l'}(2Wk_E) T_l) \, a_{al'} = i^l e^{il\theta_a} \tag{5.24}$$

We reduce the sum on l to a sum on positive integers, using the antisymmetric sin and the properties of the Bessel function.

$$\Psi_a(r, \phi) = \sqrt{\frac{2}{Wk_a}} \sum_{l=1}^{\infty} (a_{al} - (-1)^l a_{n-l}) R_l \sin(l\phi) \tag{5.25}$$

The Cartesian wavefunctions are defined as antisymmetric with respect to the x axis. Now we can match the wavefunctions in the different regions by using the relation

$$0 = \int ds \left(\Psi_a \frac{\partial}{\partial \mathbf{r}} \Psi_b - \Psi_b \frac{\partial}{\partial \mathbf{r}} \Psi_a \right) \tag{5.26}$$

We can now integrate alone the dashed line in the above sketch, the third line is on $y = W$, where the wavefunction vanish. We consider Ψ_a, the wavefunctions we have derive above in the various regions, and $\Psi_b^{\pm} = \sqrt{\frac{2}{W}} e^{\pm i k_b' x} \sin(\frac{b'\pi}{W} y)$, a general solution that we can write in both Cartesian and radial form. Writing the last equation as $I_\phi + I_y + 0 = 0$ where I_y is an

72

integral on the strait lines at $x = \pm W$, and I_ϕ is on a semidisc at $r = W$. The first integral is

$$I_y = \int_0^W \left(\Psi_a \frac{\partial}{\partial x} \Psi_b - \Psi_b \frac{\partial}{\partial x} \Psi_a \right) \Big|_{x=W} \tag{5.27}$$

$$\tag{5.28}$$

Calculating it on both sides separately, using the orthogonality of the sin

$$I_y^R = i\frac{1}{\sqrt{k_b}} \boldsymbol{S}_{ab}^T (\pm k_b - k_b) \tag{5.29}$$

$$I_y^L = i\frac{1}{\sqrt{k_a}} \delta_{ab}(\pm k_b - k_a) + i\frac{1}{\sqrt{k_b}} \boldsymbol{S}_{ab}^R (\pm k_b + k_b m) \tag{5.30}$$

The integral $I_y = I_y^L - I_y^R$ for the different signs are

$$I_y(\Psi_b^-) = -2i\sqrt{k_a}\delta_{ab} + 2i\sqrt{k_b}\boldsymbol{S}_{ab}^T \tag{5.31}$$

$$I_y(\Psi_b^+) = +2i\sqrt{k_b}\boldsymbol{S}_{ab}^R \tag{5.32}$$

For the second integral, on the dashed half circle line in the region $(0, \pi)$ we expand $\Psi_b^\pm$ in the radial basis

$$\Psi_b^\pm(r, \phi) = \sqrt{\frac{2}{W}} e^{\pm ik_b x} \sin(\frac{b\pi}{W}y) = \frac{-i}{\sqrt{2W}} \left(e^{\pm ik_b x + i(\frac{b\pi}{W})y} - e^{\pm ik_b x - i(\frac{b\pi}{L})y} \right) = \tag{5.33}$$

$$= \pm\sqrt{\frac{2}{W}} \sum_{l=-\infty}^{\infty} (\pm i)^l J_l(k_E r) e^{il\phi} \sin(l\theta_b) \tag{5.34}$$

We sum on positive integers by $J_{-l}(x) = (-1)^l J_l(x)$

$$\Psi_b^\pm(r, \phi) = \pm 2i\sqrt{\frac{2}{W}} \sum_{l=1}^{\infty} (\pm i)^l J_l(k_E r) i^l \sin(l\phi) \sin(l\theta_b) \tag{5.35}$$

The second integral is

$$I_\phi = \int_0^\pi W d\phi \left(\Psi_a \frac{\partial}{\partial r} \Psi_b - \Psi_a \frac{\partial}{\partial r} \Psi_b \right)_{r=W} \tag{5.36}$$

Substituting the wavefunctions, using the orthonormality of sin

$$I_\phi = \pm\frac{2\pi i}{\sqrt{k_a}} \sum_{l=1}^{\infty} (\pm i)^l (a_{al} - (-1)^l a_{a-l}) \sin(l\theta_b)(R_l \partial_r J_l - J_l \partial_r R_l)\Big|_{r=W} \tag{5.37}$$

Using (5.17) and the Wronskian of the Bessel functions $J_l \partial_r N_l - N_l \partial_r J_l = \frac{2}{\pi r}$ the integral is

$$I_\phi = \mp \frac{4}{\sqrt{k_a} W} \sum_{l=1}^{\infty} (\pm i)^l T_l (a_{al} - (-1)^l a_{a-l}) \sin(l\theta_b) \tag{5.38}$$

As we seen the two integral sum is zero therefore $I_y = -I_\phi$ and we can find the expressions

$$\boldsymbol{S}_{ab}^T = \delta_{ab} + \frac{2i}{\sqrt{k_a k_b} W} \sum_{l=1}^{\infty} (-i)^l T_l \sin(l\theta_b)(a_{al} - (-1)^l a_{a-l}) \tag{5.39}$$

$$\boldsymbol{S}_{ab}^R = \frac{-2i}{\sqrt{k_a k_b} W} \sum_{l=1}^{\infty} i^l T_l \sin(l\theta_b)(a_{al} - (-1)^l a_{a-l}) \tag{5.40}$$

Note that we assume a long enough waveguide so there is no incoming evanescent modes. Then the $\boldsymbol{S}$ submatrix of the open modes fully describe the open modes scattering, without any need to consider the outgoing evanescent modes.

For the matrix to satisfy the TRS condition as in section 4.7, we require that $\boldsymbol{S} = \boldsymbol{S}^{transposed}$. Each of the above submatrices fullfill that condition. The calculation for incoming particle in the oposite direction lead to the same result, hence the $\boldsymbol{S}$ matrix is of the form.

$$\boldsymbol{S} = \begin{pmatrix} \boldsymbol{S}^R & \boldsymbol{S}^T \\ \boldsymbol{S}^T & \boldsymbol{S}^R \end{pmatrix} \tag{5.41}$$

The following figures present the absolute values of four representative $\boldsymbol{S}$ matrices.
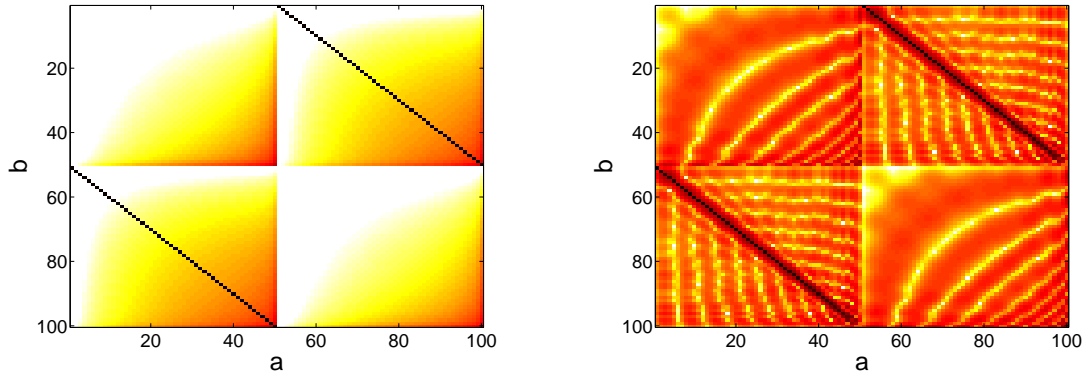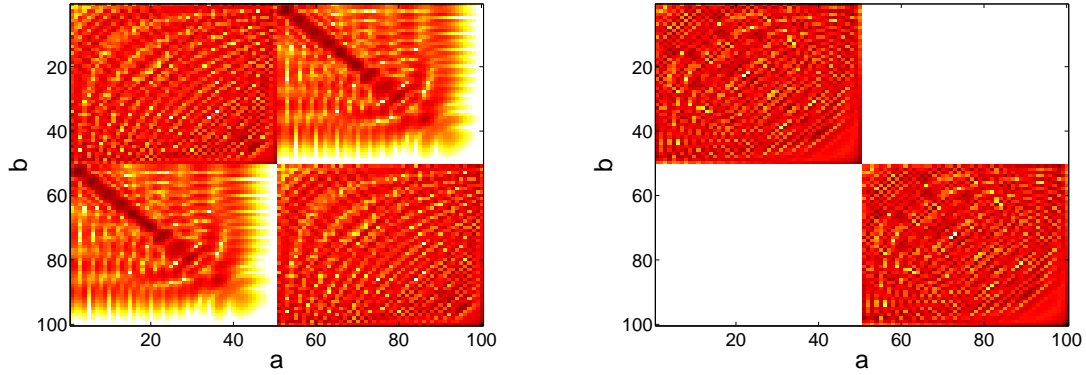
Fig.25 From left up to bottom right, $\boldsymbol{S}$ matrices for $\epsilon = 0.01, 0.1, 0.7, 1$

5.4 Classical Kubo formula and Drude

With the classical transition matrix of section 5.2 we have created the transition matrix $\boldsymbol{g}$. With its quatum counterpart $\boldsymbol{g}_{ab}^{QM} = |\boldsymbol{S}_{ab}|^2$ we can find the Landauer and Drude conductance, using Eq.(3.40) and Eq.(1.11).

In the following we plot those conductance as function of the radius ϵ.

Fig.26 The classical conductance, in log and normal scale. The dotted line and dashed line are for Landauer and Drude conductance respectively in the classical approximation. The dots are the corresponding quantum results.

5.5 System's eigenvalues

As in the network, the waveguide system is define by the scattering matrix $\boldsymbol{S}$ of previous section and the free propagation matrix $\boldsymbol{S}_W$.

$$\boldsymbol{S}_W = \begin{pmatrix} 0 & e^{ik_a L}\delta_{ab} \\ e^{ik_a L}\delta_{ab} & 0 \end{pmatrix} \tag{5.42}$$

By solving the secular equation.

$$\det[\,\boldsymbol{S}_{\mathrm{w}}\,\boldsymbol{S} - 1\,] \;\; = \;\; 0 \tag{5.43}$$
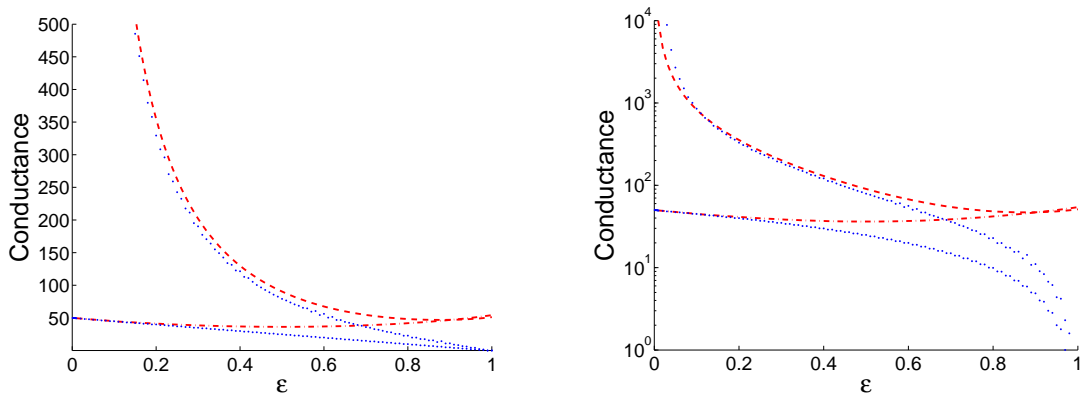
and the linear equation for the eigenstates

$$\begin{pmatrix} A_L \\ A_R \end{pmatrix} = \boldsymbol{S}_{\mathrm{w}}\,\boldsymbol{S}_{\mathrm{D}} \begin{pmatrix} A_L \\ A_R \end{pmatrix} \tag{5.44}$$

we obtain numerically for any size of ϵ a table

$$(E_n, \varphi_a^{(n)}, A_a^{(n)}) \qquad n = \text{level index} \qquad a = \text{mode index} \tag{5.45}$$

For the numerical study we have chosen a waveguide system with $\mathcal{M} = 50$ modes. We choose the length of the waveguide to be $L = 100.32$, and an energy window with $N = 400$ levels.

For each energy level n the wavefunction in the waveguide is

$$\Psi_n(x,y) = \sum_a A_a \sin(k_a^{(n)} x + \phi_a^{(n)}) \sqrt{\frac{2}{L}} \sin(a\pi y/W) \tag{5.46}$$

The semidisc system is symmetric to reflection on the disc. Therefore each eigenstate will either symmetric or anti symmetric for all modes. Therefore at $x = L/2$, point opposite to the location of the scatterer, the phase in the sin of the wavefunction will be either $\pm\pi/2$ for a symmetric wavefunction, or 0 for antisymmetric one. We found the expression for $\varphi_a^{(n)}$ at Eq.(4.53), now it is re-written as

$$\varphi_a^{\pm} \;\; = \;\; \begin{cases} -\frac{1}{2}k_a L \pm \frac{\pi}{2} & \text{For a symmetric wavefunction} \\ -\frac{1}{2}k_a L & \text{For an anti-symmetric wavfunction} \end{cases} \tag{5.47}$$

Using this structure it will more convnient to calculate the current operator not at $x = 0$ as in the previous chapter, but at $x = L/2$ where the phase of the wavefunction is simple.

In the following we plot the energy levels as a function of the reflection. If the reflection is small enough each pair of states, a symmetric state and an antisymmetric one. will be nearly degenerate. This structure will be lost as we increase the reflection.
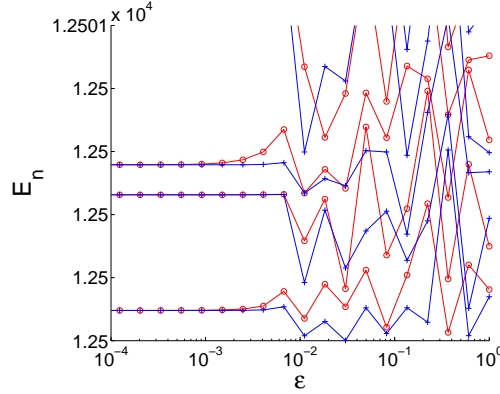
Fig.27 The energy levels within a small energy window near $E = 12500$ are shown as a function of ϵ. The circles indicate energy levels with symmetric eigenvectors. The crosses with antisymmetric levels.

In the following we plot the phases $\varphi_a^{(n)}$ and amplitudes $A_a^{(n)}$ of the system for a single energt level n, as a function of the reflection ϵ. If the reflection is small enough the wavefunction will be localize on a single mode a, in the level we choose that mode is $a = 7$. The result for that mode are indicated by crosses. We ploted the phses of the wavefunction at $x = L/2$. namely $\varphi_a^{(n)} + k_a^{(n)} L/2$, we can see that the eigenstate we chose is a symmetric one, the phase in all modes are either $\frac{\pi}{2}$ or $-\frac{\pi}{2}$. The phase in the localized mode is $\frac{\pi}{2}$.

The amplitudes have structure similar to that in section 4.6. Where the wavefunction is localized on a single mode for small reflection and become ergodic if the reflection is increase. Note that the amplitudes are multiply by $\sqrt{L/2}$, so the amplitude of the localizes mode equal 1.

Fig.28 Right panel: The phases $\varphi_a^{(n)} + k_a^{(n)} L/2$ of one representative eigenstate. The crosses indicate the phase in the mode 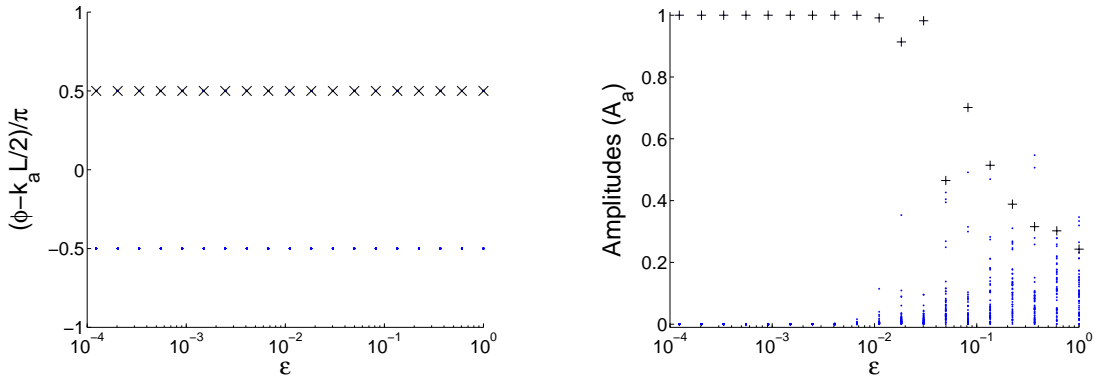$a = 7$, where most of the wavefunction is localized for $\epsilon \to 0$. Left panel: The amplitudes $A_a^{(n)}$ multiply by $\sqrt{L/2}$ for the same state as a function of ϵ. The wavefunction is localized on a single bond for small reflection and become ergodic for large reflection.

5.6   The calculation of the matrix elements

Using the the density of state in the waveguide we re-write the Kubo formula

$$G = \pi \varrho_F^2 \times \langle\langle |\mathcal{I}_{nm}|^2 \rangle\rangle \tag{5.48}$$

as $G = \langle\langle G_{nm} \rangle\rangle$, where $\langle\langle \cdot \rangle\rangle$ indicate the coarse graining procedure as in the previous chapter and

$$
\begin{aligned}
G_{nm} &= \pi \varrho_F^2 |\mathcal{I}_{nm}|^2 \tag{5.49} \\
&= \frac{e^2}{2\pi\hbar} \times \frac{W^2}{2} \left| \frac{L}{2} \sum_a k_a A_a^{(n)} A_a^{(m)} \sin(\phi_a^{(n)} - \phi_a^{(m)}) \right|^2 \tag{5.50}
\end{aligned}
$$

We can calculate those matrix elements at any point alone the ring. As explained in the previous section we will calculate it at $x = L/2$ where the phases are known. We note that for any pair of states n, m with the same symmetry the expression $\phi_a^{(n)} - \phi_a^{(m)}$ will be either 0 or π, in both case the G_{nm} matrix elements vanish.

On the other hand, for a pair of states with different symmetry this expression equal either $\pi/2$ or $-\pi/2$, depending on the symmetry of the specific mode.

In the limit $\epsilon \to 0$, we will get pairs of states, both localize on the same mode, with different symmetry. Those state are the result of the even-odd degeneracy we expect on a reflectionless single ring, the matrix elements for those pair are

$$G_{nm} = \frac{e^2}{2\pi\hbar} \times \frac{W^2}{2} k_a{}^2 \tag{5.51}$$

Where a is the localized mode. In that region other states are localized on different modes, therefore other matrix elements vanish. In order to calculate the ergodic value we remind that the amplitude for ergodic wavefunction are, as in section 3.2,

$$A_a \propto 1/\sqrt{k_a} \tag{5.52}$$

Using the normalization demand $L/2 \sum_a A_a^2 = 1$, we can find that in the ergodic limit

$$A_a^2 \approx \frac{4}{WLk_a} \tag{5.53}$$

For this calculation we assume $E \approx E_{min}$ and we replace the sum by the integral.

$$\sum_a \frac{1}{k_a} \approx \sum_a \frac{W}{\pi\sqrt{\mathcal{M}^2 - a^2}} \approx \frac{W}{\pi} \int_0^{\mathcal{M}} \frac{1}{\sqrt{\mathcal{M}^2 - a^2}} = \frac{W}{2} \tag{5.54}$$

With this results we can find the matrix elements, we can assume the phase sign is random.

$$G_{nm} = \frac{e^2}{2\pi\hbar} \times 2 \left| \sum_a \sin(\pm\pi/2) \right|^2 = 2\mathcal{M} \tag{5.55}$$

In summary the limiting values for the matric elements are.

$$G_{nm} = \frac{e^2}{2\pi\hbar} \times \begin{cases} 0 & \text{for a pair of states, localized on different modes} \\ \frac{W^2}{2} k_a{}^2 & \text{for a pair of state, localize on the same mode and have different symmetry} \\ 0 & \text{for a pair of ergodic states with the same symmetry} \\ 2\mathcal{M} & \text{for a pair of ergodic states with different symmetry} \end{cases}$$

The next plot presents the the average values of the first near diagonals as a function of the reflection. The first diagonal reach, in the limit of small reflection $\epsilon \to 0$ to the value of

$$\langle G_{n,n+1} \rangle = \frac{e^2}{2\pi\hbar} \times \frac{1}{2}\frac{W^2}{2}\langle k_a{}^2 \rangle \tag{5.57}$$

Where the $\frac{1}{2}$ indicate that in that limit half of the states are correlated on the same mode a and half are not correlated. The ergodic avarage value is $\langle G_{n,m} \rangle = \frac{e^2}{2\pi\hbar} \times \mathcal{M}$, half of the matrix elements equal zero as they have the same symmetry the other half equal $2\mathcal{M}$.
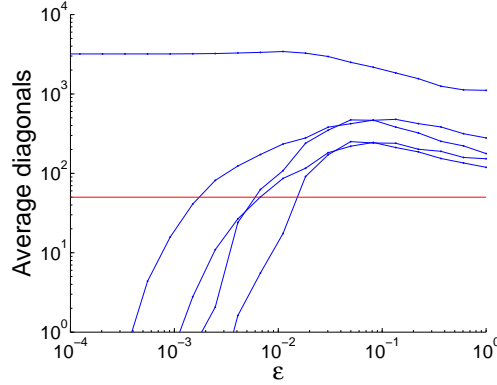
Fig.29 The average value of $G_{n,n+r}$ for $r = 1, 2, 3, 4, 5$ as a function of ϵ (doted line). The ergodic $\mathcal{M}$ value is represented with solid line.

5.7 Numerical results

With all the ingredients we can now calculate the conductance, the following are analog to Fig.17 in the previous chapter, and they dispaly similar results.
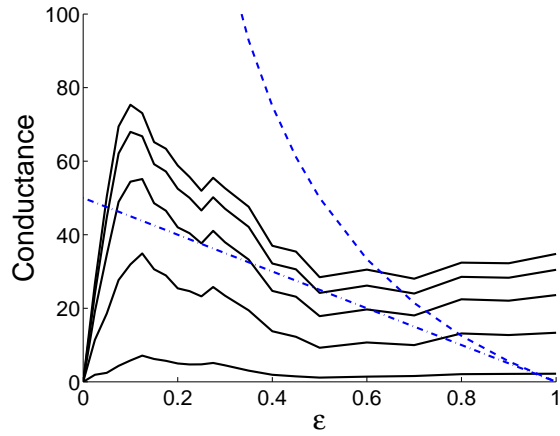
Fig.30: (a) Left panel: The mesoscopic conductance G in units of $e^2/(2\pi\hbar)$ as a function of ϵ. The curves from bottom to top are for $\gamma = 1, 2, 3, 4, 5$. The total number of open modes is $\mathcal{M} = 50$. The dotted line is G_{Landauer} while the dashed line is G_{Drude}.

In this chapter we have shown that the results obtaind in the simplistic model of the previous chapter, fit well with the realistic model we have presented.

Chapter 6

Summary

In our work we have studied the conductance of close mesoscopic system. In chapter 3 the treatment was essentially classical as we assume short coherence time. Within the framework of the scattering approach, we have found an expression for this conductance which we named the Drude conductance. This expression can be regarded as a generalization of the Landauer formula. Our starting point was the Kubo formalism, we also used a master equation for the derivation. Calculation of the conductance in waveguide with attached cavity as a general example for multimode Drude conductace has showed that the unlike the Landauer result the conductance in a closed ring is not bounded by the number of channels.

In chapter 4 we have studied the mesoscopic conductance of an essentially coherent ballistic ring. The specific calculation has been done for a network model, but all its main ingredients are completely generic. Ballistic rings are not typical "quantum chaos" systems. Their eigenfunctions are not ergodic over the whole accessible phase space and cannot be regarded as an extended "random wave". Consequently the perturbation matrix $\mathcal{I}_{nm}$ is highly structured and sparse, and the Kubo formula is no longer valid. Then one has to adopt an appropriate coarse graining procedure in order to calculate the true mesoscopic conductance.

The "averaging" over the matrix elements of the current operator should be done according to the appropriate prescription: resistor-network scheme for the mesoscopic conductance G_{meso}. which is relevant when all relaxation processes are much weaker compared with the driving in the system, and algebraic scheme for spectroscopic conductance G_{spec}. The latter correspond with the classical, Drude conductance. The calculation procedure implies that

$$G_{\mathrm{meso}} < G_{\mathrm{spec}} \leq G_{\mathrm{Drude}} \tag{6.1}$$

while our numeric further suggests that typically

$$G_{\mathrm{meso}} < G_{\mathrm{Landauer}} \tag{6.2}$$

For an optimal value of γ, such that G_{meso} is maximal, we still have $G_{\mathrm{meso}} \lesssim G_{\mathrm{Landauer}}$. Our conjecture is that this statement is true in general. We did not find a mathematical argument to establish this conjecture, except the very simple case of a single mode ballistic ring[11] where the calculations of G can be done analytically. It is still an open challenge to derive an estimate for the mesoscopic conductance in terms of g_T. It was possible to derive such an expression in the single mode case. There it was found that $G_{\mathrm{meso}} \propto (1 - g_T)^2 g_T$. In the general case ($\mathcal{M} > 1$) the calculation is more complicated.

We suspect that our expression for the participation ratio Eq.(4.56) constitutes an important step towards this goal. In any case we were not able to derive a reliable closed analytical expression. We did calculate the conductance for a larger number of $\mathcal{M}$ up to 450, Fig 16. But, We could not determine weather the conductance saturate to a limit or has some weak divergance as $\mathcal{M} \to \infty$.

Another open question is the quantum classical correspondane in the limit $g_T \to 0$. The classical Kubo calculation will result in zero conductance in that limit. However, in our quantum calculation we found that in this limit the conductance is proportional to the number of open modes.

In the chapter 5 We have tested the generality of our statements by analyzing another, more realistic model, where the ring is modeled as a waveguide with a semi-disc scatterer. We have found the $\boldsymbol{g}$ matrix for this model and calculate the Drude and Landauer conductance. We also found the $\boldsymbol{S}$ matrix for this model and calculate the mesoscopic and spectroscopic conductance. We have verified that the pertubation matrix elements has roughly the same expected dependence on g_T as in our simple model of chapter 4. And verified that the results for the mesoscopic conductance are qualitatively the same in both cases.

Note that in Both the semi-disc model, and the network model, that the participation ratio does not exhibit anomalous saturation as typical, say, for a "star graph" [24].

It should be emphasized that if the mesoscopic conductance that we have discussed apply only when there is neither a very effective relaxation nor a decoherence process. In the presence of such effect one can justify, depending on the circumstances, either the use of the traditional Kubo-Drude result, or the use of the Landauer result.

Appendix A

Numerical routines

The numerical work was done using Matlab routines. the main routine is called *Network_system.m*. This is the primary routine, it define the input variables of the model. It accept as input the number of open modes $\mathcal{M}$, k_{min}, k_{max} which are lowest and highest value of wavenumber k. And a list of reflection sizes r_T, which is define as

$$r_T = 1 - g_T \tag{A.1}$$

The routine construct J, a permutation matrix that describe connection of the bonds in the system. And $L = diag(L_a)$, diagonal matrix of the lengths of the bonds. The lengths of the bond are random number in the region $(1.1, 0.9)$. Both matrices are $2\mathcal{M} \times 2\mathcal{M}$ For example for $\mathcal{M} = 2$ those matrices will be

$$
J = \begin{pmatrix} 0 & 0 & 1 & 0 \\ 0 & 0 & 0 & 1 \\ 1 & 0 & 0 & 0 \\ 0 & 1 & 0 & 0 \end{pmatrix} \qquad L = \begin{pmatrix} 1.034 & 0 & 0 & 0 \\ 0 & 0.987 & 0 & 0 \\ 0 & 0 & 1.034 & 0 \\ 0 & 0 & 0 & 0.987 \end{pmatrix} \tag{A.2}
$$

Using the input variables The routine calculate N the number of levels to be found and Nr the number of reflection sizes.

Then the routine runs a 'for' loop for all reflection sizes. for each size of the reflection it calls the functions $S\_matrix.m$, $Find.m$ and $CreateInm.m$.

The $S\_matrix.m$ function create the S matrix of the scatterer, as specify in section 4.1. The function take as input the reflection size.

$Find.m$ is a function created by Rosenberg [41] it find a set of eigenvalues k_n in the specify region that solve the secular equation of 4.35, and find the corresponding eigenvectors $A_{La}^{(n)}$ and $A_{Ra}^{(n)}$ of 4.33 for each level n and mode a. The function input is the matrices S, L, J and the k limits k_{min} and k_{max}. Note that

$$\mathbf{S}_D \;\; = \;\; S \tag{A.3}$$

$$\mathbf{S}_W \;\; = \;\; Je^{ikL} \tag{A.4}$$

Where $\mathbf{S}_D$ and $\mathbf{S}_W$ are define at 4.31 4.32. The combined matrix $\mathbf{S}_W\mathbf{S}_D$ in the equation is created by the sub routine $Umatrix.m$.

Now the main routine call the function $CreateInm.m$. This function use the output of $Find.m$ and the L matrix to calculate the amplitude and phase of 4.52 and 4.53. It also use those variables to calculate the PR of 4.54 and the matrices elements I_{nm} and $\bar{I}_{nm}$ of 4.57 and 4.58.

After the loop the routine call the function $DataAnalysis.m$, it use r_T, M, and the matrices elements I_{nm} and $\bar{I}_{nm}$ to calculate the various types of conductance. Namely, G_{meso}, both as it define in 4.27 and as define in 4.28, G_{spec}, as it define in 4.29, $G_{Landauer}$ as it was calculated at 1.14 and G_{Drude} as it was calculated at 1.15.

In the following table we plot the variable, there names in the routines, there matrices sizes and a description for each of them.
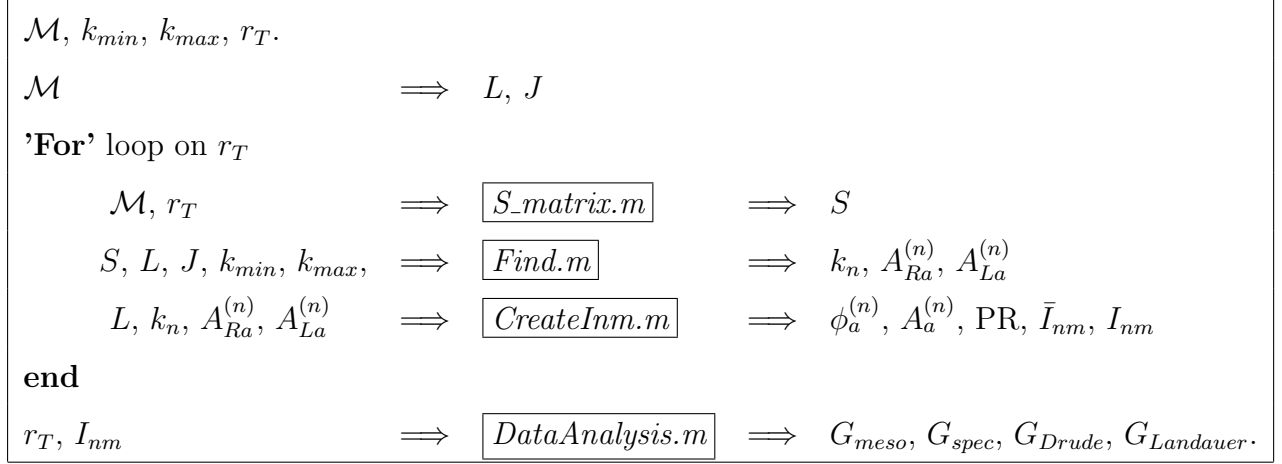
|			
$\mathcal{M}$	*Input.Channels*	Scalar	Number of Open modes
k_{max}	*Input.kmax*	Scalar	Lowest k_n
k_{min}	*Input.kmin*	Scalar	Highest k_n
r_T	*Input.a*	$1 \times Nr$	Reflection size
J	*Input.J*	$2\mathcal{M} \times 2\mathcal{M}$	Permutation matrix
L	*Input.L*	$2\mathcal{M} \times 2\mathcal{M}$	Bond lengths
N	*Input.N*	Scalar	Number of levels
Nr	*Input.Nr*	Scalar	Number of sizes r_T
S	*Input.S*	$2\mathcal{M} \times 2\mathcal{M}$	S matrix
k	*Output.k*	$1 \times N$	Eigenvalues
n	*Output.n*	$1 \times N$	Eigenvalues indices
$A_{La}^{(n)}, A_{La}^{(n)}$	*Output.Amplitude*	$N \times 2\mathcal{M}$	Eigenvectors
$A_a^{(n)}$	*Output.NormalizeAmplitudes*	$N \times \mathcal{M}$	Amplitudes
$\phi_a^{(n)}$	*Output.phi*	$N \times \mathcal{M}$	phases
IPR	*Output.IPR*	$1 \times N$	IPR$= (\text{PR})^{-1}$
I_{nm}	*Output.Inm*	$N \times N$	
$\bar{I}_{nm}$	*Output.Cnm*	$N \times N$	
G_{Drude}	*Output.G_Drude*	$1 \times Nr$	
$G_{Landauer}$	*Output.G_land*	$1 \times Nr$	
G_{meso}	*Output.Gmeso*	$1 \times Nr$	
G_{meso}	*Output.Gha*	$1 \times Nr$	Harmonic average
G_{spec}	*Output.Gspec*	$1 \times Nr$	

Other, technical variables are

Input.kTol	The tolerance in the k values
Input.k0	describe the zero value for k

A block diagram of the main routine:

Network_system

$\mathcal{M}$, k_{min}, k_{max}, r_T.					
$\mathcal{M}$	$\Longrightarrow$	L, J			
'For' loop on r_T					
$\quad\quad\mathcal{M}$, r_T	$\Longrightarrow$	$\boxed{S\_matrix.m}$	$\Longrightarrow$	S	
$\quad\quad S$, L, J, k_{min}, k_{max},	$\Longrightarrow$	$\boxed{Find.m}$	$\Longrightarrow$	k_n, $A_{Ra}^{(n)}$, $A_{La}^{(n)}$	
$\quad\quad L$, k_n, $A_{Ra}^{(n)}$, $A_{La}^{(n)}$	$\Longrightarrow$	$\boxed{CreateInm.m}$	$\Longrightarrow$	$\phi_a^{(n)}$, $A_a^{(n)}$, PR, $\bar{I}_{nm}$, I_{nm}	
end					
r_T, I_{nm}	$\Longrightarrow$	$\boxed{DataAnalysis.m}$	$\Longrightarrow$	G_{meso}, G_{spec}, G_{Drude}, $G_{Landauer}$.	

In chapter 5 we have calculate the conductance in a waveguide closed to a ring instead of the network model. The numerics equire some trivial modification which are not elaborated. We only add the numerical calculation of the S matrix which is describe in 5.3. This routine use the energy E and the semidisc radius ϵ to calculate the S matrix of the system.

$$E, \epsilon \quad \Longrightarrow \quad \boxed{semidisc.m} \quad \Longrightarrow \quad S$$
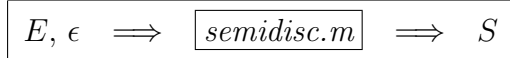
These are the printouts of the routines.

A.1   Network_system.m

```
clear global Input Output
clear Result_Outputs
global Input Output
Input.a=exp(-10:.5:0);
% Number of Channels
Input.Channels = 50;
% Number of Energy levels
Input.N = 200;
Input.Nr=length(Input.epsilon);
% L
l=1+.1*(1-2*rand(1,N));
L=diag([l,l]);
```

```matlab
Input.L = L_matrix(Input.Channels,range);
% J
Input.J = [zeros(Input.Channels, Input.Channels), eye(Input.Channels);
           eye(Input.Channels), zeros(Input.Channels, Input.Channels)];
% The handle to the function that updates returns U(E)
Input.UMatrix =@UMatrix;
% The tolerance in k
Input.kTol = 1e-3;
Input.kmin = 2000;
Input.kmax = Input.kmin+pi*Input.N/Input.Channels;
Input.k0=0;
for j=1:Input.Nr;
    clear global Output
    global Output
    tic;
    Input.S=S_matrix(Input.epsilon(j),Input.Channels);
    Output.S=Input.S;
    % Find routine
    Find;
    % CreateInm routine
    CreateInm;
    Result_Outputs(j)=Output;
end
DataAnalysis(Input,Result_Outputs)
save([date,'-d'])
```

A.2   S_matrix.m

```matlab
function S=S_matrix(epsilon,N)

for n=1:N
    for m=1:N
        R(n,m)= sqrt( epsilon /N) * exp(2*pi*i*(n*m)/N);
        if (n==m)
            T(n,m)=sqrt(1-epsilon);
        end
    end
end
S=[R,T;T,-R'];
```

A.3 Find.m

```
global Input Output
% Find the total length of the system
Output.TotalLength = trace(Input.L);
% Calculate Phi(k0)
Input.Phi0 = sum(Angle(eig(Input.UMatrix(Input.k0))));
% Save S(k0)^dagger
Input.S0dag = conj(Input.S);
% The length of the segments we will divide (Input.kmin,Input.kmax) into.
dk = 2*pi/(Output.TotalLength);
% Initialize the number of k's found so far
Output.NumFound = 0;
% Initialize the result arrays
Output.k = [];
Output.n = [];
Output.Amplitudes = [];
% Initialize the counter that counts the number of runs of Lions
Output.Runs = 0;
% The first time the loop runs, we make as if there was a segment that
% ended at Input.kmin
n2 = n(Input.kmin);
% The beginning of the first interval
BeginInterval = Input.kmin;
% Initialize the end of the first interval, to make sure that we enter the
% while loop
EndInterval = 0;
% The main loop: for every interval
% While there is still another interval to work on
while(EndInterval < Input.kmax)
   % If we are within dk of Input.kmax
   if (Input.kmax - BeginInterval) < dk
       % End the interval at Input.kmax
       EndInterval = Input.kmax;
   else
       % The interval is of length dk
       EndInterval = BeginInterval + dk;
     end;
          % The new level numbers of the limits of the segment
   n1 = n2;
   n2 = n(EndInterval);
     % If there is at least one k in the current segment
```

```matlab
    if (n2 - n1) > Input.nTol
        % Increment the runs counter
        Output.Runs = Output.Runs + 1;
                % Find the k's in this segment, by using binary search
        Lions(BeginInterval, EndInterval, n1, n2);
    end;
    % The beginning of the next interval
    BeginInterval = BeginInterval + dk;
end; % End of main loop
% If the draw flag is set, display the results
if Input.Draw > 0
    % Display the results
    disp(['Number of k''s found: ' num2str(Output.NumFound)]);
    disp(['Number of Runs (Lions): ' num2str(Output.Runs)]);
    disp('k:')
    disp(Output.k)
    disp('n:')
    disp(Output.n)
    disp(['Time elapsed: ' num2str(toc) ' sec.']);
end;
% Output the variables
evalin('base', 'global Input Output');
%%%%%%%%%%%%%%%%%%%%%%%%%%%%%%%%%%%%%%%%%%%%%%%%%%%%%%%%%%%%%%%%%%%%%%%%%%%%%

function Lions(k1, k2, n1, n2)
% Lions finds k's in a given range.
% (k1, k2) is the range to look in
% (n1, n2) are the "level numbers" that correspond to k1 and k2 (note that
% they are not necessarily whole!)
global Input Output
% If the segment is of length kTol or smaller
if (k2-k1) <= Input.kTol
    % The k's we have found
    Currentk = (k1+k2)/2;
    % The number of the level
    Currentn = n2;
    % If we need to calculate the amplitudes
    if Input.CalculateAmplitudes
        % Get the eigenvectors and eigenvalues
        [EigenVectors, SingularValues] = eig(Input.UMatrix(Currentk));
        EigenValues = diag(SingularValues);
    end;
```

```matlab
% Find the number of k's in this segment.
% If Input.nTol is much smaller than the real size of the jump, we
% might get the wrong value here.
NumKs = floor((n2-n1)/Input.nTol);
% For each k in this segment
for j=1:NumKs
    % Increment the number of k's found
    Output.NumFound = Output.NumFound + 1;
     % If we need to calculate the amplitudes
    if Input.CalculateAmplitudes
        % We want to find the eigenvector that corresponds to the eigenvalue
        % that has an angle closest to 0
        % Choose only the eigenvalues with real > 0
        Filter = real(EigenValues)>0;
                    % Find their absolute imaginary part
        AbsImag = abs(imag(EigenValues(Filter)));
        % This gives us the final filter = real > 0 and min imaginary
        % part
        Filter = (abs(imag(EigenValues)) == min(AbsImag)) & real(EigenValues)>0;
         % Store the eigenvector
        %ADDED when the degeneracy is exact numerically we will
        %use to distinguish eigenvalues, choosing only the first one.
        if sum(Filter)>1
            Filter2=zeros(length(Filter),1);
            Filter2(min(find(Filter)))=1;
            Filter=Filter2==1;
        end
       Output.Amplitudes(:, Output.NumFound) = EigenVectors(:, Filter);
        % If there is more than one root, get rid of the eigenvector and
        % eigenvalue that we have already stored.
        % The reason for this is that if there are n k's in this segment,
        % we must get n different eigenvectors.
        if (NumKs>1)
            try,
                EigenVectors = EigenVectors(:, ~Filter);
                EigenValues = EigenValues(~Filter);
            catch,
                error(['Lions:NumOfEigenVectors', ...
                    'The number of eigenvectors found was larger than' ...
                    'expected. \n You probably need to make Input.nTol'...
                    'closer to the real size of the jump, or make' ...
                    'Input.kTol smaller.'])
```

```
                  end;
            end;                         end;
                 % Save the k and level number
        Output.k(Output.NumFound) = Currentk;
        Output.n(Output.NumFound) = Currentn;
    end;
    % There is nothing left to do, so return
    return;
end;
% Find the k and n for the middle of this segment
k12 = (k1+k2)/2;
n12 = n(k12);
% If there are k's in the left half
if (n12 - n1) > Input.nTol
    % Increment the runs counter
    Output.Runs = Output.Runs + 1;
    % Invoke Lions on the left half
    Lions(k1, k12, n1, n12);
end;
% If there are k's in the right half
if (n2 - n12) > Input.nTol
    % Increment the runs counter
    Output.Runs = Output.Runs + 1;
    % Invoke Lions on the right half
    Lions(k12, k2, n12, n2);
end;
%%%%%%%%%%%%%%%%%%%%%%%%%%%%%%%%%%%%%%%%%%%%%%%%%%%%%%%%%%%%%%%%%%%%%%%%%%%
function n = n(k)

% n calculates the number of the level associated with k
global Input Output
% Calculate Phi (the sum of thetas)
Phi = sum(Angle(eig(Input.UMatrix(k))));
% This term must be calculated in advance, so that we can get rid of
% possible jumps of 2*pi resulting from the difference in definition of
% the range of angles ([-pi, pi] as opposed to [0, 2*pi])
Y = imag(log(det(Input.S0dag*Input.S)));
if Y < -Input.NumericalError
    Y = Y + 2*pi;%
end;
% The number of the level.
% We use abs to get rid of tiny imaginary parts that sometimes show up.
```

```
n = abs((Input.Phi0-Phi+(k-Input.k0)*Output.TotalLength+Y)/(2*pi));
%%%%%%%%%%%%%%%%%%%%%%%%%%%%%%%%%%%%%%%%%%%%%%%%%%%%%%%%%%%%%%%%%%%%%%%%%%%
function phi = Angle(z)
% Angle finds the phase angle of z in the [0,2*pi] segment
% z is a scalar or vector
% Get the components of z
re = real(z);
im = imag(z);
% Find theta
theta = atan(im./re);
% For each element of z
for j=1:length(z)
    % According to the quadrant, find phi
    % Left half
    if (re(j) < 0)
        phi(j) = pi + theta(j);
    % Right half
    else
        % First quadrant
        if (im(j) > 0)
            phi(j) = theta(j);
        % Fourth quadrant
        else
            phi(j) = 2*pi + theta(j);
         end;
    end;
end;
```

A.4   Umatrix.m

```
function UE = UMatrix(k)
global Input Output

% Calculate U(k) for this k, and return it
UE = Input.J*expm(i*k*Input.L)*Input.S;
```

A.5   CreateInm.m

```
global Input Output

Nm=Output.NumFound;
```

```matlab
Output.phi=zeros(1,Nm);
Output.IPR=zeros(1,Nm);
NormalizeFactor=zeros(1,Output.NumFound);
for n=1:Output.NumFound;
    %for each energy level
    for a=1:Input.Channels;
        %for each mode
        %calculate phi, depend on the mode and channel, claculate
        %separately for each mode and channel
        phi=angle(Output.Amplitudes(a+Input.Channels,n)/Output.Amplitudes(a,n));
        %The new amplitude, after gauge.
        NewAmplitude(a,n)=2*abs(Output.Amplitudes(a,n));
        Output.teta(a,n)=mod(-Output.k(n)*Input.L(a,a)/2+phi/2+pi/2,pi);
        %calculate the Amplitude factor, the factor is calculated for each
        %channel seperatley.
        NormalizeFactor(n)=NormalizeFactor(n)+...
            NewAmplitude(a,n)^2*(Input.L(a,a)/2+...
            sin(2*Output.teta(a,n))/(4*Output.k(n))-sin(2*(Output.teta(a,n)+...
            Output.k(n)*Input.L(a,a)))/(4*Output.k(n)) );
    end
    %calculate the normalize amplitude
    Output.NormalizeAmplitude(:,n)=NewAmplitude(:,n)./sqrt(NormalizeFactor(n));
    %The IPR
    for a=1:Input.Channels;
    Output.IPR(n)=Output.IPR(n)+(Output.NormalizeAmplitude(a,n)^2*Input.L(a,a)/2 )^2;
    end
    Localized_mode=find(max(abs(Output.NormalizeAmplitude(:,n))) ==...
    abs(Output.NormalizeAmplitude(:,n)));
    Output.Localized_psi1(n)=...
    angle(Output.Amplitudes(Localized_mode+Input.Channels,n)...
    /Output.Amplitudes(Localized_mode,n));
    Output.Localized_psi2(n)=Output.k(n)*Input.L(Localized_mode,Localized_mode);
    Output.Localized_teta(n)=...
    mod(-Output.Localized_psi2(n)/2+Output.Localized_psi1(n)/2+pi/2,pi);
end
Inm=zeros(Nm);
Cnm=zeros(Nm);
%for each energy level
for n=1:(Nm);
    for m=1:(Nm);
        if 1%(abs(n-m)<Input.Channels)
            for a=1:Input.Channels;
```

```
                    Cnm(n,m)=Cnm(n,m)+Input.L(a,a)/2*Amplitude(a,n)*Amplitude(a,m);
                    Inm(n,m)=Inm(n,m)+Input.L(a,a)/2*Amplitude(a,n)*Amplitude(a,m)*...
                        sin(teta(a,n)-teta(a,m));
                end
                Output.Inm(n,m)=abs(Inm(n,m))^2;
                Output.Cnm(n,m)=abs(Cnm(n,m))^2;
            end
        end
end
Output.q_E=zeros(1,length(Inm));
for n=1:Nm;
    Output.mean_IPR=mean(Output.IPR(filter));
end
```

A.6   DataAnalysis.m

```
function DataAnalysis(Input,Result_Outputs)
Nr=Input.Nr;
close all
gamma=[1,2,3,4,5];
for k=1:length(gamma);
    N=Input.N-5;
    for j=1:Nr;
        Inm=Result_Outputs(j).Inm(1:N,1:N);
        F=zeros(length(Inm));
        for n=1:length(Inm)
            for m=1:length(Inm)
                if (n~=m)
                F(n,m)=1/(n-m).^2*1/gamma(k)*exp(-2*abs((n-m)/gamma(k)));
                end
            end
        end
        g_nm=2*Input.Channels^2*Inm.*F;
        S=ones(length(g_nm),1)*sum(g_nm);
        g_nm=g_nm-eye(length(g_nm)).*S;
        I=zeros(length(g_nm),1);
        I(length(g_nm))=-1;
        I(1)=1;
        V=pinv(g_nm)*I;
        Output.Gmeso(j)=1/(V(length(V))-V(1))*length(V);
        %%%%G2 issue - simplify recipe
        alg_sum=zeros(1,length(Inm));
```

```
        for n=1:length(Inm)
            for m=1:n
                alg_sum(n)=alg_sum(n)+(m-n)^2*g_nm(n,m);
         end     end
        Output.Gha(j)= 1/sum(1./alg_sum(2:length(Inm)))*length(V);
        %%%%Gspec issue - harmonic->algebric
         alg_sum=zeros(1,length(Inm));
         for n=1:length(Inm)
            for m=1:n
                alg_sum(n)=alg_sum(n)+(m-n)^2*g_nm(n,m);
            end
        end
        Output.Gspec(j)=sum(alg_sum(2:length(Inm)))/length(V);
    end
end
Output.G_land=Input.Channels.*(1-Input.epsilon);
Output.G_drude=Input.Channels.*(1-Input.epsilon)./Input.epsilon;
```

A.7   semidisc.m

```
function S=semidisc(E,a)
    mass=1;
    L=1;
    size=floor(L/pi *sqrt(2*mass*E));
    lSize=l_size(a,size);
    lvalmin=lSize.*ones(size);
    k=sqrt(2*mass*E);
    r=zeros(size);
    t=zeros(size);
    for l=1:lSize;
        Tvec(l)=T(l,k,a);
    end
    for n=1:size;
        kvec(n)=sqrt( k^2-(n*pi/L)^2 );
    end
    [Fmatb,Fmatc]= Fmatrix(k,a,lSize,Tvec);
    Rmat=R(k,kvec,size,lSize);
    for n=1:size;
        [b,c]=b(Fmatb,Fmatc,Rmat,lSize,n);
         for m=1:size;
            Sumlt=0;
            Sumlr=0;
```

```matlab
            lt=zeros(1,lSize/2);
            lr=zeros(1,lSize/2);
            for l=2:2:(lSize);
                lt(l/2)=Tvec(l)*b(l)*(Rmat(m,lSize+1+l)-Rmat(m,lSize+1-l))
                    +Tvec(l-1)*c(l-1)*(Rmat(m,lSize+1+(l-1))+Rmat(m,lSize+1-(l-1)));
                lr(l/2)=-Tvec(l)*b(l)*(Rmat(m,lSize+1+l)-Rmat(m,lSize+1-l))
                    +Tvec(l-1)*c(l-1)*(Rmat(m,lSize+1+(l-1))+Rmat(m,lSize+1-(l-1)));
            end
            Sumlt=sum(lt);
            Sumlr=sum(lr);
            r(n,m)=1/(L*sqrt((kvec(n))*((kvec(m)))))*Sumlr;
            t(n,m)=1/(L*sqrt((kvec(n))*((kvec(m)))))*Sumlt;
        end
    end
    S=[(r),(t)+eye(n);(t)+eye(n),(r)];
%%%%%%%%%%%%%%%%%%%%%%%%%%%%%%%%%%%
function [b,c]=b(Fmatb,Fmatc,Rmat,lSize,n)

    Rvecb=zeros(lSize,1);
    Rvecc=zeros(lSize,1);

    %vector of R_n,-l - R_n,l
    for l=1:lSize;
            Rvecb(l)=Rmat(n,lSize+1-l)-Rmat(n,lSize+1+l);
            Rvecc(l)=Rmat(n,lSize+1-l)+Rmat(n,lSize+1+l);
    end
    b=inv(Fmatb)*Rvecb;
    c=inv(Fmatc)*Rvecc;
%%%%%%%%%%%%%%%%%%%%%%%%%%%%%%%%%%%
function  [Fmatb,Fmatc]=Fmatrix(k,a,lSize,Tvec)
    L=1;
    %create the matrix
    Fmatb=zeros(lSize);
    Fmatc=zeros(lSize);
    %filling all the possibile values for the structure function, there
    for l3=-lSize:2:lSize*2;
        StrucFun(l3+lSize+1)=SF(2*L*k,l3);
    end
     for l1=1:lSize;
     for l2=1:lSize;
      Fmatb(l1,l2)=(l1==l2) + ( StrucFun(l1+l2+lSize+1)-StrucFun(l1-l2+lSize+1) )*Tvec(l2);
      Fmatc(l1,l2)=(l1==l2) - ( StrucFun(l1+l2+lSize+1)+StrucFun(l1-l2+lSize+1) )*Tvec(l2);
```

```matlab
     end
    end
%%%%%%%%%%%%%%%%%%%%%%%%%%%%%%
function Rmat=R(k,kvec,size,lsize)
    mass=1;
    L=1;
    for n=1:size
        for l=-lsize:1:lsize;
      %  Rmat(n,lsize+l+1)=( (-sign(l)*i*kn(n)+n*pi/L)/k )^(abs(l)) ;
          Rmat(n,lsize+l+1)=i^l*exp(-i*l*(pi-acos(kvec(n)/k))) ;
        end
    end
%%%%%%%%%%%%%%%%%%%%%%%%%%%%%%%%%%%%%%%%%%
function T=T(l,k,a)
    rho=pi-atan(-besselj(l,k*a)/bessely(l,k*a));
    %rho=pi-atan( - (besselj(l-1,k*a)-besselj(l+1,k*a))/(bessely(l-1,k*a)-bessely(l+1,k*a))
    %rho=pi-rho;
    T=i*exp(i*rho)*sin(rho);
    %T=-besselj(l,k*a)/(besselj(l,k*a)+i*bessely(l,k*a));
%%%%%%%%%%%%%%%%%%%%%%%%%%%%%%%%%%%%%%%%%%
function F = SF(x,l)
%the structure function F
    M=50;
    L=1;
    if ( l/2==round(l/2) )
        %only for even l
        for n=1:M;
            F1(n)=(besselj(l,x*n));
            F2(n)=(bessely(l,x*n));
        end
        for n=(M-20):1:M;
            J(n)=sum(F1(1:n));
            Y(n)=sum(F2(1:n));
        end
        rst1=mean(J((M-20):M));
        rst2=mean(Y((M-20):M));
        f=rst1+i*rst2;
        F=2*f*cos(pi*l/2);
    else
        F=0;
    end
```

Bibliography

[1] D. Cohen and Y. Etzioni, J. Phys. A **38**, 9699 (2005).

[2] Y. Etzioni, S. Bandopadhyay and D. Cohen, cond-mat/0607746

[3] S. Bandopadhyay, Y. Etzioni, and D. Cohen, cond-mat/0603484

[4] M. Buttiker, Y. Imry and R. Landauer, Phys. Lett. **96A**, 365 (1983).

[5] R. Landauer and M. Buttiker, Phys. Rev. Lett. **54**, 2049 (1985). M. Buttiker, Phys. Rev. B **32**, 1846 (1985).

[6] Y. Imry and N.S. Shiren, Phys. Rev. B **33**, 7992 (1986).

[7] Y. Gefen and D. J. Thouless, Phys. Rev. Lett. **59**, 1752 (1987).

[8] M. Wilkinson, J. Phys. A **21** (1988) 4021.

[9] A. Kamenev and Y. Gefen, Int. J. Mod. Phys. **B9**, 751 (1995).

[10] Measurements of conductance of closed diffusive rings are described by B. Reulet M. Ramin, H. Bouchiat and D. Mailly, Phys. Rev. Lett. **75**, 124 (1995).

[11] D. Cohen, T. Kottos and H. Schanz, cond-mat/0505295.

[12] M. Wilkinson, B. Mehlig and D. Cohen, "Semilinear response", **cond-mat/0512070**, to be published in Europhysics Letters (2006).

[13] D. Cohen, Annals of Physics **283**, 175 (2000).

[14] M. Wilkinson and E.J. Austin, J. Phys. A **23**, L957 (1990).

[15] M. V. Berry, J. Phys. A 10, 2083 (1977)

[16] E. J. Heller, Phys. Rev. Lett. 53, 1515 (1984)

[17] E. B. Bogomolny, Physica D 31, 169 (1988)

[18] O. Agam and S. Fishman, Phys. Rev. Lett. 73, 806 (1994)

[19] A Bäcker, R Schubert, J. Phys. A: Math. Gen, 1999

[20] A. I. Shnirelman, Usp. Mat. Nauk 29, 181 (1974);

[21] L. Kaplan and E. J. Heller, Annals of Physics 264, 171 (1998)

[22] L. Kaplan and E. J. Heller, Phys. Rev. E 63, 066214 (2001)

[23] G Berkolaiko, JP Keating, B Winn, Phys. Rev. Lett. 91, 134103 (2003)

[24] H. Schanz and T. Kottos, Phys. Rev. Lett. **90**, 234101 (2003).

[25] S. Datta, *Electronic Transport in Mesoscopic Systems* (Cambridge University Press 1995).

[26] Y. Imry, *Introduction to Mesoscopic Physics* (Oxford Univ. Press 1997), and references therein.

[27] C. Jarzynski, Phys. Rev. E **48**, 4340 (1993).

[28] D. Cohen, Phys. Rev. B 68, 155303 (2003).

[29] D. Stone and A. Szafer, http://www.research.ibm.com/journal/rd/323/ibmrd3203I.pdf

[30] D. Cohen, Phys. Rev. B 68, 201303(R) (2003).

[31] For mini-review and further references see: D. Cohen, "Quantum pumping and dissipation in closed systems", Proceedings of the conference "Frontiers of Quantum and Mesoscopic Thermodynamics" (Prague, July 2004), to be published in Physica E. http://www.bgu.ac.il/∼dcohen/ARCHIVE/pme.pdf.

[32] D. Cohen, unpublished

[33] The Γ issue is discussed in Section VIII of [28]

[34] T. Kottos and U. Smilansky. Phys. Rev. Lett. **79**, 4794 (1997).

[35] R. Blümel and U.Smilansky, Physica D **36** (1989) 111-136.

[36] H. Schanz and U. Smilansky, Chaos, Solitons & Fractals **5**, (1995) 1289-1309.

[37] N.F. Mott, Phil. Mag. **22**, 7 (1970).

[38] N.F. Mott and E.A. Davis, Electronic processes in non-crystalline materials, (Clarendon Press, Oxford, 1971).

[39] D. Cohen, T. Kottos and H. Schanz, Phys. Rev. E **71**, 035202(R) (2005).

[40] F.M.Izrailev, T.Kottos and G.P.Tsironis, J.Phys. C **8**, 2823 (1996).

[41] G. Rosenberg and D. Cohen, J. Phys. A 39, 2287 (2006).

[42] Edwards and Thouless, J.Phys.C 5 807 (1972)

ההולכה בטבעות בליסטיות
The conductance of ballistic rings

<u>חיבור לשם קבלת תואר "מגיסטר" בפקולטה למדעי הטבע</u>

מוגש על ידי: יואב עציוני

המנחה: פרופ׳ דורון כהן

אוניברסיטת בן גוריון בנגב
הפקולטה למדעי הטבע
המחלקה   לפיסיקה

25 דצמבר 2006

הסטודנט:	תאריך:
אישור המנחה:	תאריך:
אישור יו״ר הועדה המחלקתית:	תאריך:

מוליכות Landauer. ההולכה של מערכות מזוסקופיות פתוחות, שווה, בגבול הפיזור החלש למספר הערוצים הפתוחים. בעבודה זו נשאל מה תהיה ההולכה אם נסגור המערכת לטבעת? האם היא עדיין תהיה חסומה על ידי מספר הערוצים הפתוחים? מצאנו שתי תשובות עבור שאלה זו. הראשונה [1] ישימה אם אנו מניחים זמן קוהרנטיות קצר, ולכן הטיפול הינו קלסי במהותו. תוך שימוש בגישת פיזור אנו מוצאים ביטוי עבור מוליכות זו אותה כינינו מוליכות Drude. כמו כן נבחין בין סוגים שונים של השפעות סביבתיות וננתח מודל עבור מפזר ספציפי ונדגים כי בניגוד להולכה במערכות פתוחות במערכות סגורות ההולכה איננה חסומה על ידי מספר הערוצים.

בחלקה השני של העבודה [2] נניח טבעת קוהרנטית במהותה, שבה הנעה גורמת להרחבת רמות חלשה, וכתוצאה מכך בליעת אנרגיה נוצרת עקב מעברי רמות של חוק הזהב של פרמי. אנו מוצאים כי אם תהליכי רפיה כתוצאה מהסביבה הינם מאוד חלשים בהשוואה להנעה, התוצאה תהיה סוג חדש של מוליכות שנכנה אותה מוליכות מזוסקופית. מוליכות זו היא חלשה בהרבה בהשוואה לתוצאה הקלסית, הדבר נובע ממאפיינים לא אוניברסליים של מטריצת ההפרעה. מאפיינים אלו הינם רכיב גנרי במערכות קוונטיות כאוטיות.

המוליכות מוגדרת דרך חוק ג'אול, כמקדם קצב בליעת האנרגיה. המאפיינים הלא אוניברסליים במטריצת ההפרעה יכולים ליצור צוורי בקבוק המקטינים את בליעת האנרגיה. אנו מוצאים את ההולכה באמצעות אנלוגיה עם בעית הפרקולציה, אלא שבמקרה זה הפרקולציה הינה במרחב האנרגיה. אנו מבחינים בין המוליכות המזוסקופית הזו לבין המוליכות הספקטרוסקופית הגדולה ממנה בהרבה שנוצרת כאשר תהליכי הרפייה הינם חזקים.

בחלק השלישי של העבודה אנו מוודאים את הכלליות של מסקנותינו על ידי ניתוח מודל ריאליסטי שבו הטבעת רבת הערוצים ממודלת כמוליך גל עם מפזר בצורת חצי מעגל.